Spotila, 2012: Data Repository

Methods

Figure DR-1 (a-d) illustrates conceptually how divide elevation depends on the geometry of intersecting ridges. Ridgeline slope depends on both hillside gradient and the obliquity of opposing hillside trends. The simple relationship between ridgeline slope and hillside obliquity for varying hillside gradients (Fig. DR-1c) is based on the simplifying assumption of planar hillsides, although natural hillsides generally exhibit curvature in 3D. The height, shape, and dynamic evolution of ridgelines will also depend on the competition of relative advance of opposing hillsides (Fig. DR-1d).

In the global survey, groups of peaks worldwide were screened using *GoogleEarth*. Peaks were selected based on regional hierarchies (i.e. top highest peaks in a given area), such as the top 100 peaks in the world (Table 1). The peaks screened are listed in Table DR-1 (n=255), along with location coordinates. The locations span a range of erosional (glacial and fluvial), climatic (arid to humid), and tectonic (erosion and uplift rates) settings. Lists of top peaks in different areas were based on various websites, primarily including Wikipedia and PeakBagger:

http://en.wikipedia.org/wiki/List_of_highest_mountains

http://www.peakbagger.com/ListIndx.aspx

Although these are un-refereed internet sources, all coordinates of peaks listed were checked and the elevation verified using *GoogleEarth*. Minor errors in these lists, such as missing peaks or specific values of prominence, cannot be completely ruled out. However, the intention of using these regional hierarchies was to eliminate bias in which peaks were selected for inspection in the global survey. All peaks in these lists were screened and included in Table DR-1, regardless of appearance, and all peaks in these lists are significant, prominent peaks in their respective areas. Note that peak prominence is defined as the height of a peak above the lowest contour that encircles it and nothing higher (Fig. DR-1e). Prominence is typically set at ~5-10% of the total local relief of a range (e.g. ~500 m in the high Himalaya; Table 1), such that many high peaks may not be included in the list because they are too close in elevation to a nearby higher peak. Figure DR-1f shows a comparison of a parabolic ridge with only one prominent peak relative to a ridge with lower saddles that yields many more prominent peaks. As an aside, the frequency of prominent peaks per area may actually be an interesting metric for comparison of mountain topography.

Peaks were screened using unexaggerated 3D visualization of digital topography (on a template combining satellite imagery) using *GoogleEarth* at a uniform scale of approximately 1:10,000. *GoogleEarth* uses a variety of elevation data, ranging from 10 m to 90 m resolution (SRTM data). In most mountain ranges examined, the resolution was 10 m or 30 m. Regardless of the DEM resolution, however, the *GoogleEarth* was adequate for identifying ridges shorter than ~0.5 km at all locations at 1:10,000 scale. Spatial variation in DEM resolution should thus not affect the results of the global survey. Peaks located within 0.2 km of divide intersections were classified as divide-junction peaks (Fig. DR-2). The contributing divides had to be a minimum of ~0.5 km long and separate tributary valleys by at least 1 km. This threshold was designed to include divides that separate first-order drainages, but to exclude minor rill-like crenulations along hillsides within individual basins. An additional criteria was that divide-junction peaks had to appear with three (or more) hillside faces that clearly drain into separate basins with clear concave contours. Examples of peaks that were classified as ridge-only (vs. divide-junction) based on this criteria are shown in Fig. DR-3.

Most divide-junction peaks consist of divide triple junctions, although a significant fraction of quadruple junctions also occur (Table DR-1). The minimum lengths of contributing divides were measured in map view for each location (Table DR-1). Since the goal of the survey was to identify peaks that have at least three intersecting divides, the third-shortest contributing divide was measured for all divide junctions (i.e. not the absolute minimum on quadruple junctions). The distribution of these third-shortest divide lengths shows that 3/4 of the divide-junction peaks are made by divides that exceed 3 km length (Fig. 2). Where the shortest-contributing divide length exceeds 5-10 km, length measurements may be ambiguous due to the possibility of taking multiple paths off of the divide network (Figure DR-1g).

The relationship between peak and divide-junction locations was also tested at the local scale. Ten primarily glacial and fluvial areas of rugged topography were selected for examination of drainage divide structure in map and/or profile view (Table DR-2; Fig. DR-4, DR-5). Note that some of the glacial areas are now deglaciated, but exhibit topography that is characteristically glacial. Similarly, the highest elevations of some of the fluvial areas may have experienced minor glacial or periglacial influence during the last glacial maximum (e.g. the Atlas Mountains), but the topography of these ranges is dominantly fluvial. The areas mapped exclude volcanic terrain, low-relief areas, and high-relief areas that exhibit interfluves with relict surfaces. Sources for the long-term denudation rates reported for these areas are provided in Table DR-2. Results of profile and map-view analysis are presented in Tables DR-3 and DR-4.

Divide maps were constructed using shaded relief images from *GoogleMaps*. All maps were shaded from the northwest and mapped at 1:200,000 scale on a graphical interface. Divides were easy to identify using this interface, given that side illumination highlights most ridges as white lines. Given that ridges and divides exhibit semi-fractal distributions and that the resolution of DEMs may vary by location, a mapping threshold of minimum ridge size was employed; only divides >5 km long and separated by >3 km (i.e. valley spacing) were mapped. Mapped ridges also had to have significant relief from hillsides and separate clearly-developed basins with curved contours. This criteria made mapping of ridges somewhat subjective, but was used to screen out topographic crenulations along individual hillsides that do not separate first or higher order basins. Divide junctions were mapped for each area based on the mapped ridge networks. Where two triple junctions came within ~1 km of each other, they were combined into a quadruple junction. Various statistics of the occurrence of divide junctions and total divide length per mapped area are reported in Table DR-4. When counting divide junctions in each area, quadruple junctions were counted twice (given that each is equivalent to 2 triple junctions joined together).

Five glacial and fluvial areas were selected for ridge profile analysis (Table DR-3, Fig. DR-5). Ridge profiles were constructed using *GoogleEarth* in the same geographic interface as the global peak survey, but at a uniform scale of ~1:20,000. Elevations were sampled at approximately 1-km spacing, so that only significant peaks and undulations are represented. This spacing was selected to reduce data volume, given that the profiles would eventually be analyzed at small scale only. The elevations of all divide junctions were also directly sampled. Ridge profiles follow the irregular trace of ridges in map view and include all ridges in a connected ridge network using the criteria listed above for ridge maps. Profiles generally cover 80-km-long primary ridges, and thus do not cover the entire area of each map. In some cases, profiles stop abruptly mid-ridge, because a profile was stopped after a representative length had been obtained. Secondary ridges are plotted as extending in either the positive or negative x-direction depending on the orientation of the primary ridge and the side from which the secondary ridge joins (Fig. DR-5). Several ridge profiles were constructed using 1:250,000 topographic maps (Chugach, St. Elias, Smoky Mtns., San Gabriel Mountains), but corrected for the same pattern of ridges as the *GoogleEarth* profiles. Once completed, divide junctions were identified and compared to peak locations. The divide junctions on profiles are identical to those on the maps of the same area, given that they share defining criteria. Peaks were defined as any positive relief form, regardless of prominence. The slope of primary ridges was calculated between each elevation spacing and thus has a wavelength of 1 km and may miss slight undulations. The topographic roughness was measured in two ways; $\boldsymbol{\Psi}_1$ is the horizontal ridge length divided by the total ridge length in profile (i.e. akin to sinuosity, but measured in profile at 8x exaggeration), and $\boldsymbol{\Psi}_2$ is the normalized distance of the ridge profile over which 50% of the profile's relief is obtained.

This study was made possible by the easily-used geographic tools provided by *Google*. GoogleEarth and GoogleMaps enable instant access to global topography, without having to download and process numerous individual patches of DEMs. Although the association of peaks and ridge junctions has previously been observed Gilbert, 1880; Twidale, 1976; Gonzalez, 2003), recognition of the influence of drainage divide structure on peaks required the advent of easily accessible digital topography.

Table DR-1: Global survey of peaks.

GROUP 1: Top-100 peaks in the world (500 m prominence), all of which are above the glacial limit.

Rank	Name	Elev. (m)	Region	Location	Shortest Ridge	Peak type
1	Everest	8848	Himalaya	27.9881 N, 86.9253 E	5.2	*triple*
2	K2	8611	Karakoram	35.8814 N, 76.5133 E	6.5	*five-sided tower*
3	Kangchenjunga	8586	Himalaya	27.7033 N, 88.1475 E	15.3	*triple*
4	Lhotse	8516	Himalaya	27.9617 N, 86.9331 E	9.6	*triple*
5	Makalu	8485	Himalaya	27.8897 N, 87.0889 E	8.0	*triple*
6	Cho Oyu	8188	Himalaya	28.0942 N, 86.6608 E	3.3	*triple, almost quad.*
7	Dhaulagiri	8167	Himalaya	28.6967 N, 83.4931 E	16.6	*quad.*
8	Manaslu	8163	Himalaya	28.5500 N, 84.5597 E	5.5	*triple*
9	Nanga Parbat	8126	Himalaya	35.2372 N, 74.5892 E	0.9	*triple*
10	Annapurna I	8091	Himalaya	28.5956 N, 83.8203 E	4.6	*triple*
11	Gasherrum I	8080	Karakoram	35.7244 N, 76.6964 E	8.7	*triple*
12	Broad Peak	8051	Karakoram	35.8106 N, 76.5683 E		***ridge only***
13	Gasherbrum II	8034	Karakoram	35.7578 N, 76.6533 E		***ridge only***
14	Shishapangma	8027	Himalaya	28.3533 N, 85.7786 E	1.3	*triple*
15	Gyachung Kang	7952	Himalaya	28.0981 N, 86.7450 E	5.3	*triple*
16	Annapurna II	7937	Himalaya	28.5347 N, 84.1219 E	3.5	*triple*
17	Gasherbrum IV	7932	Karakoram	35.7606 N, 76.6161 E	9.6	*triple*
18	Himalchuli	7893	Himalaya	28.4367 N, 84.6397 E	23.5	*triple*
19	Distaghil Sar	7884	Karakoram	36.3258 N, 75.1878 E	28.9	*triple*
20	Ngadi Chuli	7871	Himalaya	28.5033 N, 84.5667 E	1.4	*triple*
21	Nuptse	7864	Himalaya	27.9675 N, 86.8869 E	0.8	*triple*
22	Khunyang Chhish	7823	Karakoram	36.2053 N, 75.2078 E	6.6	*quad.*
23	Masherbrum	7821	Karakoram	35.6411 N, 76.3058 E	6.8	*quad.*
24	Nanda Devi	7816	Himalaya	30.3758 N, 79.9708 E	1.6	*triple*
25	Chomo Lonzo	7804	Himalaya	27.9306 N, 87.1078 E	4.5	*triple, almost quad.*
26	Batura Sar	7795	Karakoram	36.5103 N, 74.5225 E		***ridge only***
27	Kanjut Sar	7790	Karakoram	36.2056 N, 75.4169 E	15.1	*five-sided tower*
28	Rakaposhi	7788	Karakoram	36.1425 N, 74.4894 E	17.7	*triple*
29	Namche Barwa	7782	Himalaya	29.6311 N, 95.0553 E	23.2	*triple*
30	Kamet	7756	Himalaya	30.9200 N, 79.5917 E	3.5	*triple*
31	Dhaulagiri II	7751	Himalaya	28.7628 N, 83.3883 E	14.1	*triple*
32	Saltoro Kangri	7742	Karakoram	35.3992 N, 76.8481 E	3.4	*quad.*
33	Jannu	7711	Himalaya	27.6822 N, 88.0444 E	1.6	*triple*
34	Tirich Mir	7708	Hindu Kush	36.2553 N, 71.8417 E	11.8	*triple*
35	Molamenqing	7703	Himalaya	28.3550 N, 85.8097 E	2.6	*quad.*
36	Gurla Mandhata	7694	Himalaya	30.4386 N, 81.2967 E	12.8	*triple*
37	Saser Kangri I	7672	Karakoram	34.8667 N, 77.7525 E	23.4	*triple*
38	Chogolisa	7665	Karakoram	35.6131 N, 76.5747 E	3.6	*triple*
39	Kongur Tagh	7649	Kunlun	38.5933 N, 75.3133 E	1.6	*triple*
40	Dhaulagiri V	7618	Himalaya	28.7339 N, 83.3614 E	10.9	*triple*
41	Shispare	7611	Karakoram	36.4406 N, 74.6808 E	17.2	*quad.*
42	Trivor	7577	Karakoram	36.2875 N, 75.0850 E	6.1	*triple*
43	Gangkhar Puensum	7570	Himalaya	28.0472 N, 90.4553 E	5.3	*triple*
44	Gongga Shan	7556	Daxue Shan	29.5953 N, 101.8797 E	22.0	*quad.*
45	Annapurna III	7555	Himalaya	28.5850 N, 83.9900 E	37.4	*triple*
46	Muztagh Ata	7546	Kunlun	38.2758 N, 75.1161 E	7.7	*quad.*
47	Skyang Kangri	7545	Himalaya	35.9264 N, 76.5675 E	1.0	*triple*
48	Changtse	7543	Himalaya	28.0247 N, 86.9142 E	5.0	*quad.*
49	Kula Kangri	7538	Himalaya	28.2269 N, 90.6164 E	7.3	*triple*
50	Kongur Tiube	7530	Kunlun	38.6158 N, 75.1958 E	9.5	*triple*
51	Mamostong Kangri	7516	Karakoram	35.1419 N, 77.5775 E	2.0	*triple*
52	Saser Kangri II	7513	Karakoram	34.8047 N, 77.8067 E	4.8	*triple*
53	Ismail Sarmani	7495	Pamir	38.9431 N, 72.0158 E	16.0	*triple*
54	Saser Kangri	7495	Karakoram	34.8456 N, 77.7850 E		***ridge only (cone)***
55	Noshaq	7492	Hindu Kush	36.4322 N, 71.8286 E		***ridge only***
56	Pumari Chhish	7492	Karakoram	36.2114 N, 75.2503 E	1.4	*triple*
57	PaGu Sar	7476	Karakoram	36.4878 N, 74.5878 E	13.7	*triple*
58	Yukshin Gardan Sar	7469	Karakoram	36.2511 N, 75.3747 E	2.1	*triple*
59	Teram Kangri I	7462	Karakoram	35.5800 N, 77.0783 E		***ridge only***
60	Jongsong Peak	7462	Himalaya	27.8817 N, 88.1358 E	30.0	*triple*
61	Malubiting	7458	Karakoram	36.0033 N, 74.8753 E	13.6	*triple*
62	Gangapurna	7455	Himalaya	28.6050 N, 83.9636 E	4.5	*triple*
63	Jengish Chokusu	7439	Tian Shan	42.0347 N, 80.1297 E	30.0	*triple*
64	K12	7428	Karakoram	35.2958 N, 77.0222 E	10.3	*triple*
65	Yangra	7422	Himalaya	28.3914 N, 85.1272 E	26.4	*triple*
66	Sia Kangri	7422	Karakoram	35.6633 N, 76.7617 E	3.5	*triple*
67	Momhil Sar	7414	Karakoram	36.3178 N, 75.0364 E	10.1	*triple*
68	Kabru N	7412	Himalaya	27.6339 N, 88.1167 E	3.7	*triple*

69	Skil Brum	7410	Karakoram	35.8508 N, 76.4286 E	14.9	*quad.*
70	Haramosh	7409	Karakoram	35.8400 N, 74.8975 E	10.9	*triple*
71	Istor-o-Nal	7403	Hindu Kush	36.3756 N, 71.8983 E	2.1	*triple, nested*
72	Ghent Kangri	7401	Karakoram	35.5178 N, 76.8006 E	12.6	*triple*
73	Ultar Sar	7388	Karakoram	36.3908 N, 74.7167 E	5.6	*triple*
74	Rimo I	7385	Karakoram	35.3550 N, 77.3689 E	5.0	*triple*
75	Churen Himal	7385	Himalaya	28.7347 N, 83.2175 E	0.6	*triple*
76	Teram Kangri III	7382	Karakoram	35.5997 N, 77.0481 E	3.9	*quad.*
77	Sherpi Kangri	7380	Karakoram	35.4661 N, 76.7814 E	2.5	*triple*
78	Labuche Kang	7367	Himalaya	28.3042 N, 86.3508 E	9.2	*triple*
79	Kirat Chuli	7362	Himalaya	27.7878 N, 88.1953 E	3.9	*triple*
80	Abi Gamin	7355	Himalaya	30.9325 N, 79.6025 E	11.9	*quad.*
81	Nangpai Gosum	7350	Himalaya	28.0733 N, 86.6142 E	7.0	*triple*
82	Saraghrar	7349	Hindu Kush	36.5475 N, 72.1150 E	4.3	*triple, nested*
83	Chamlang	7321	Himalaya	27.7750 N, 86.9797 E	3.5	*triple*
84	Chongtar	7315	Karakoram	35.9153 N, 76.4292 E	6.8	*quad., nested*
85	Baltoro Kangri	7312	Karakoram	35.6392 N, 76.6733 E	2.1	*triple*
86	Siguang Ri	7309	Himalaya	28.1472 N, 86.6850 E	6.5	*triple*
87	The Crown	7295	Karakoram	36.1067 N, 76.2058 E	1.2	*quad. (cone)*
88	Gyala Peri	7294	Himalaya	29.8144 N, 94.9686 E	6.8	*triple*
89	Porong Ri	7292	Himalaya	28.3894 N, 85.7200 E		***ridge only***
90	Baintha Brakk	7285	Karakoram	35.9475 N, 75.7533 E		***ridge only***
91	Yutmaru Sar	7283	Karakoram	36.2264 N, 75.3672 E	5.1	*triple*
92	Baltistan Peak (K6)	7282	Karakoram	35.4183 N, 76.5517 E	23.7	*triple*
93	Kangpenqing	7281	Himalaya	28.5508 N, 85.5456 E		***ridge only***
94	Muztagh Tower	7276	Karakoram	35.8278 N, 76.3611 E		***ridge only***
95	Diran	7266	Karakoram	36.1203 N, 74.6617 E	20.4	*quad.*
96	Labuche Kang III	7250	Himalaya	28.3014 N, 86.3839 E	11.5	*triple*
97	Putha Hiunchuli	7246	Himalaya	28.7478 N, 83.1461 E	24.0	*quad.*
98	Apsarasas Kangri	7245	Karakoram	35.5386 N, 77.1486 E	4.5	*triple*
99	Rimo III	7233	Karakoram	35.3753 N, 77.3617 E	3.7	*triple*
100	Langtan Lirung	7227	Himalaya	28.2561 N, 85.5169 E	5.1	*triple*

# of ridge-only peaks = 10. Triple/quad peaks = 90%

GROUP 2: 50 highest peaks in North America (500 m prominence), all of which are or have been glaciated.

Rank	Name	Elev. (m)	Region	Location	Shortest Ridge	Peak type
1	Mt. McKinley	6194	Alaska Range	63.0690 N, 151.0063 W	19.1	*triple*
2	Mt. Logan	5956	St. Elias Range	60.5666 N, 140.4072 W	11.2	*triple*
3	Citlaltepetl	5635	Mexico	19.0305 N, 97.2698 W		*volcano*
4	Mt. St. Elias	5489	St. Elias Range	60.2927 N, 140.9307 W	17.4	*quad.*
5	Pococatepetl	5410	Mexico	19.0225 N, 98.6278 W		*volcano*
6	Mt. Foraker	5304	Alaska Range	62.9605 N, 151.3992 W	14.8	quad.
7	Mt. Lucania	5260	St. Elias Range	61.0215 N, 140.4661 W	10.5	*triple*
8	Iztaccihuatl	5230	Mexico	19.1792 N, 98.6419 W		*volcano*
9	King Peak	5173	St. Elias Range	60.5834 N, 140.6561 W	8.8	*triple*
10	Mt. Bona	5044	St. Elias Range	61.3845 N, 141.7529 W	32.9	*triple*
11	Mt. Steele	5020	St. Elias Range	61.0929 N, 140.3118 W	15.4	*quad.*
12	Mt. Blackburn	4996	Wrangell Mtns.	61.7305 N, 143.4031 W	11.7	*volcano (eroded)*
13	Mt. Sanford	4949	Wrangell Mtns.	62.2132 N, 144.1292 W		*volcano*
14	Mt. Wood	4860	St. Elias Range	61.2323 N, 140.5139 W	7.9	*triple*
15	Mt. Vancouver	4812	St. Elias Range	60.3589 N, 139.6980 W	9.0	*triple*
16	Mt. Slaggard	4742	St. Elias Range	61.1723 N, 140.5869 W	22.4	*triple*
17	Nevado de Toluca	4690	Mexico	19.1020 N, 99.7676 W		*volcano*
18	Mt. Fairweather	4671	St. Elias Range	58.9064 N, 137.5265 W	13.5	*triple*
19	Mt. Hubbard	4557	St. Elias Range	60.3189 N, 139.0719 W	6.6	*triple*
20	Mt. Bear	4520	St. Elias Range	61.2834 N, 141.1433 W	7.4	*triple*
21	Mt. Walsh	4506	St. Elias Range	61.0034 N, 140.0172 W	3.2	*triple*
22	Mt. Hunter	4442	Alaska Range	62.9496 N, 151.0921 W	6.4	*triple*
23	Matlalcueyetl	4430	Mexico	19.2302 N, 98.0316 W		*volcano*
24	Mt. Whitney	4421	Sierra Nevada	36.5786 N, 118.2920 W	1.2	*quad.*
25	Mt. Alverstone	4420	St. Elias Range	60.3519 N, 139.0752 W	33.1	*triple*
26	University Peak	4410	St. Elias Range	61.3272 N, 141.7867 W	3.6	*triple*
27	Mt. Elbert	4401	Sawatch R., CO	39.1178 N, 106.4454 W	4.2	*triple*
28	Mt. Massive	4398	Sawatch R., CO	39.1875 N, 106.4757 W	2.5	*triple*
29	Mt. Harvard	4397	Collegiate Pks., CO	38.9244 N, 106.3207 W	2.8	*triple*
30	Mt. Ranier	4394	Cascade Range	46.8521 N, 121.7579 W		*volcano*
31	Mt. Williamson	4386	Sierra Nevada	36.6559 N, 118.3111 W	8.3	*quad.*
32	McArthur Peak	4380	St. Elias Range	60.6061 N, 140.2160 W	4.1	*triple*
33	La Plata Peak	4379	Collegiate Pks., CO	39.0294 N, 106.4729 W	3.2	*triple*
34	Blanca Peak	4374	Sangre de Cristo R., CC	37.5775 N, 105.4857 W	6.6	*quad.*
35	Uncompahgre Peak	4365	San Juan R., CO	38.0717 N, 107.4621 W	0.9	*triple*

36	Creston Peak	4359	Sangre de Cristo, CO	37.9668 N, 105.5855 W	6.0	*quad.*
37	Mt. Lincoln	4357	Mosquito R., CO	39.3515 N, 106.1116 W	2.0	*triple*
38	Castle Peak	4352	Elk Mtns., CO	39.0097 N, 106.8614 W	12.4	*quad.*
39	Grays Peak	4352	Front R., CO	39.6339 N, 105.8176 W	4.4	*quad.*
40	Mt. Antero	4351	Sawatch R., CO	38.6741 N, 106.2462 W	4.2	*triple*
41	Mt. Evans	4348	Front R., CO	39.5883 N, 105.6438 W	0.8	*triple*
42	Longs Peak	4346	Front R., CO	40.2550 N, 105.6151 W	5.5	*triple*
43	Mt. Wilson	4344	San Miguel Mtns., CO	37.8391 N, 107.9916 W	3.6	*quad.*
44	White Mountain Pk.	4344	White Mtns., CA	37.6341 N, 118.2557 W	9.9	*triple*
45	North Palisade	4343	Sierra Nevada, CA	37.0943 N, 118.5147 W		***ridge only***
46	Mt. Princeton	4329	Collegiate Pks., CO	38.7492 N, 106.2424 W	4.2	*triple*
47	Mt. Yale	4329	Collegiate Pks., CO	38.8442 N, 106.3138 W	3.9	*triple*
48	Mt. Shasta	4322	Cascade Range, CA	41.4092 N, 122.1949 W		*volcano*
49	Maroon Pk.	4317	Elk Mtns., CO	39.0708 N, 106.9890 W	20.3	
50	Mt. Wrangell	4317	Wrangell Mtns.	62.0059 N, 144.0187 W		*volcano*

9 peaks are constructional; 1 peak is ridge-only. Triple/quad = 98%.

GROUP 3: Top 20 peaks of European Alps (~100 m prominence); all are above the glacial limit

Rank	**Name**	**Elev. (m)**	**Region**	**Location**	**Shortest Ridge**	**Peak type**
1	Mont Blanc	4808	Alps	45.8336 N, 6.8650 E	4.7	*triple*
2	Monte Rosa	4634	Alps	45.9368 N, 7.8671 E	2.3	*triple*
3	Zumsteinspitze	4563	Alps	45.9319 N, 7.8714 E	1.2	*triple*
4	Dom	4545	Alps	46.0950 N, 7.8600 E	3.7	*quad.*
5	Liskamm	4527	Alps	45.9225 N, 7.8356 E	2.9	*triple*
6	Weisshorn	4506	Alps	46.1017 N, 7.7161 E	4.5	*triple*
7	Matterhorn	4478	Alps	45.9764 N, 7.6583 E	4.2	*quad.*
8	Dent Blanche	4356	Alps	46.0342 N, 7.6119 E	29.8	*quad.*
9	Nadelhorn	4327	Alps	46.1088 N, 7.8642 E	7.3	*triple*
10	Grand Combin	4314	Alps	45.9375 N, 7.2992 E	12.5	*triple*
11	Lenzspitze	4294	Alps	46.1046 N, 7.8684 E	3.0	*triple*
12	Finsteraarhorn	4274	Alps	46.5375 N, 8.1260 E	1.7	*triple*
13	Zinalrothorn	4221	Alps	46.0647 N, 7.6900 E	7.4	*quad.*
14	Grandes Jorasses	4208	Alps	45.8689 N, 6.9881 E	2.5	*triple*
15	Alphubel	4206	Alps	46.0629 N, 7.8639 E	1.2	*triple*
16	Rimpfischhorn	4199	Alps	46.0231 N, 7.8839 E	0.5	*triple*
17	Strahlhorn	4190	Alps	46.0132 N, 7.9018 E	3.7	*quad.*
18	Dent d'Herens	4171	Alps	45.9701 N, 7.6051 E		***ridge only***
19	Breithorn	4164	Alps	45.9411 N, 7.7472 E	1.1	*triple*
20	Jungfrau	4158	Alps	46.5368 N, 7.9626 E	4.0	*triple*

# of ridge-only peaks = 1. Triple/quad peaks = 95%

GROUP 4: Highest non-volcanic peaks of countries/Islands of SE Asia and Pacific; all fluvial.

Rank	**Name**	**Elev. (m)**	**Region**	**Location**	**Shortest Ridge**	**Peak type**
1	Mt. Wilhelm	4509	Papua NG	5.8000 S, 145.0333 E	7.8	*quad.*
2	Gunung Kinabalu	4095	Borneo	6.0724 N, 116.5616 E		***ridge only (rounded)***
3	Yushan	3952	Taiwan	23.4700 N, 120.9573 E	9.1	*quad.*
4	Phou Bia	2819	Laos	18.9796 N, 103.1515 E	10.4	*quad.*
5	Jirisan	1915	South Korea (mainland	35.3370 N, 127.7167 E	3.8	*triple*
6	Hokusuihaku-san	2522	North Korea (non-volc.	40.7105 N, 127.7505 E	8.5	*triple*
7	Doi Inthanon	2565	Thailand	18.5922 N, 98.4867 E	5.3	*triple (but rounded)*
8	Phnom Aural	1813	Cambodia	12.0333 N, 104.1667 E	6.9	*triple*
9	Fansipan	3143	Vietnam	22.3033 N, 103.7750 E	8.7	*triple*
10	Pulag	2922	Luzon	16.5971 N, 120.8995 E	1.4	*triple*

1 peak is ridge-only. Triple/quad = 90%.

GROUP 5: Highest peaks (5) in Australia and highest peaks (5) in Victoria, AU (all fluvial)

Rank	**Name**	**Elev. (m)**	**Region**	**Location**	**Shortest Ridge**	**Peak type**
1	Mt. Koscuiszko	2228	New South Wales	36.4559 S, 148.2633 E		***ridge only (rounded)***
2	Mt. Townsend	2209	New South Wales	36.4228 S, 148.2586 E	6.9	*triple (low relief)*
3	Mt. Twynam	2196	New South Wales	36.3933 S, 148.3147 E	3.0	*quad. (low relief)*
4	Rams Head	2190	New South Wales	36.3930 S, 148.3150 E	2.9	*triple (low relief)*
5	Jagungal	2061	New South Wales	36.1486 S, 148.3877 E		***ridge only (rounded)***
6	Mt. Bagong	1986	Victoria	36.7333 S, 147.3060 E	3.8	*quad.*
7	Mt. Feathertop	1922	Victoria	36.8948 S, 147.1365 E	4.8	*triple*
8	Mt. Hotham	1861	Victoria	36.9759 S, 147.1312 E	1.6	*quad.*
9	Mt. McKay	1849	Victoria	36.8745 S, 147.2431 E	0.9	*triple (low relief)*
10	Mt. Buller	1805	Victoria	37.1448 S, 146.4257 E		***ridge only***

3 peaks are ridge-only. Triple/quad = 70%.

GROUP 6: Highest non-volcanic peaks of countries in Central/South America (* = glacial)

Rank	Name	Elev. (m)	Region	Location	Shortest Ridge	Peak type
1	Cerro Chirripo	3820	Costa Rica	9.4841 N, 83.4887 W	8.7	*triple*
2	Mogoton	2107	Nicaraugua	13.7629 N, 86.3985 W	2.9	*triple*
3	Cristobal Colon*	5700	Colombia	10.8383 N, 73.6867 W	22.7	*quad.*
4	Bolivar	4981	Venezuela	8.5411 N, 71.0465 W	5.3	*quad.*
5	Neblina	2994	Brazil	0.8005 N, 66.0075 W	6.0	*quad.*
6	Cerro Pero	842	Paraguay	25.9017 N, 56.1600 W	5.7	*triple*
7	Aconcagua*	6962	Argentina	32.6534 S, 70.0111 W	12.1	*quad.*
8	Picos de Barroso*^	5142	Andes, Arg/Chile	34.2868 S, 70.0332 W	12.6	*triple*
9	Yerupaja*	6635	Peru	10.2687 S, 76.9056 W	2.7	*triple*
10	Illimani*	6438	Bolivia	16.6333 S, 67.7908 W	4.5	*quad.*
	^approximate highest non-volcanic					

No peaks are ridge-only. Triple/quad = 100%.

GROUP 7: All peaks over 1500 m with prominence>150 m in the San Gabriel Mtns., CA (all fluvial)

Rank	Name	Elev. (m)	Region	Location	Shortest Ridge	Peak type
1	Mt. San Antonio	3051	San Gabriel Mtns.	34.2891 N, 117.6462 W	15.0	*quad.*
2	Pine Mt.	2947	San Gabriel Mtns.	34.3137 N, 117.6443 W	8.2	*triple*
3	Dawson Pk.	2914	San Gabriel Mtns.	34.3033 N, 117.6362 W	4.9	*triple*
4	Mt. Baden Powell	2862	San Gabriel Mtns.	34.3585 N, 117.7646 W	4.5	*triple*
5	Throop Pk.	2786	San Gabriel Mtns.	34.3506 N, 117.7992 W	5.4	*quad.*
6	Telegraph Pk.	2738	San Gabriel Mtns.	34.2616 N, 117.5985 W	4.2	*quad.*
7	Cucamonga Pk.	2703	San Gabriel Mtns.	34.2226 N, 117.5853 W	6.7	*triple*
8	Ontario Mt.	2651	San Gabriel Mtns.	34.2277 N, 117.6241 W		***ridge only***
9	Timber Mt.	2522	San Gabriel Mtns.	34.2448 N, 117.5935 W	2.2	*quad.*
10	Mt. Williamson	2516	San Gabriel Mtns.	34.3754 N, 117.8639 W	0.9	*triple*
11	Mt. Islip	2508	San Gabriel Mtns.	34.3452 N, 117.8399 W	2.0	*triple*
12	Waterman Mt.	2445	San Gabriel Mtns.	34.3364 N, 117.9368 W		***ridge only (rounded)***
13	Iron Mtn.	2438	San Gabriel Mtns.	34.2884 N, 117.7134 W	4.3	*quad.*
14	no name	2432	San Gabriel Mtns.	34.3898 N, 117.9092 W	3.6	*triple*
15	Pallett Mtn.	2372	San Gabriel Mtns.	34.3856 N, 117.8855 W	1.4	*triple*
16	Twin Peks East	2364	San Gabriel Mtns.	34.3159 N, 117.9267 W	0.9	*triple*
17	Kratka Ridge	2290	San Gabriel Mtns.	34.3469 N, 117.8991 W	1.7	*triple*
18	Table Mtn.	2281	San Gabriel Mtns.	34.3824 N, 117.6851 W		***ridge only***
19	Winston Peak	2270	San Gabriel Mtns.	34.3578 N, 117.9359 W		***ridge only (rounded)***
20	Pacifico	2163	San Gabriel Mtns.	34.3820 N, 118.0346 W	7.0	*triple*
21	Mt. Gleason	1989	San Gabriel Mtns.	34.3762 N, 118.1769 W	9.0	*triple*
22	Bare Mt.	1924	San Gabriel Mtns.	34.3469 N, 117.9925 W	3.8	*triple*
23	Strawberry Pk.	1878	San Gabriel Mtns.	34.2835 N, 118.1206 W	0.8	*quad.*
24	San Gabriel Pk.	1857	San Gabriel Mtns.	34.2435 N, 118.0984 W	1.6	*quad.*
25	Mt. Lawlor	1814	San Gabriel Mtns.	34.2706 N, 118.1039 W	1.5	*quad.*
26	Sunset Pk.	1767	San Gabriel Mtns.	34.2167 N, 117.6894 W	0.7	*triple*
27	Rattlesnake Pk.	1763	San Gabriel Mtns.	34.2719 N, 117.7769 W	3.3	*quad.*
28	Mt. Wilson	1739	San Gabriel Mtns.	34.2239 N, 118.0615 W	7.4	*triple*
29	Iron Mtn.	1716	San Gabriel Mtns.	34.3488 N, 118.2292 W	2.6	*quad.*
30	Condor Peak	1651	San Gabriel Mtns.	34.3256 N, 118.2193 W	4.3	*triple*
31	Josephine Pk.	1643	San Gabriel Mtns.	34.2870 N, 118.1542 W	2.5	*triple*
32	Monrovia Pk.	1640	San Gabriel Mtns.	34.2138 N, 117.9685 W	6.3	*triple*
33	Mt. Lukens	1542	San Gabriel Mtns.	34.2691 N, 118.2391 W	3.7	*triple*
34	Snow Mt.	1508	San Gabriel Mtns.	34.3958 N, 118.2720 W	1.7	*triple*
35	Magic Mtn.	1484	San Gabriel Mtns.	34.3865 N, 118.3293 W	3.2	*quad.*
36	Yerba Buena Ridge	1181	San Gabriel Mtns.	34.3042 N, 118.2983 W	2.9	*quad.*

4 peaks are ridge-only. Triple/quad = 89%.

GROUP 8: All peaks with prominence >500 m in the Mt. Everest area of Himlaya (see Figure) (all glacial)

Rank	Name	Elev. (m)	Region	Location	Shortest Ridge	Peak type
1	Everest	8848	Himalaya	27.9881 N, 86.9253 E	5.2	*triple*
2	Lhotse	8516	Himalaya	27.9617 N, 86.9331 E	9.6	*triple*
3	Makalu	8485	Himalaya	27.8897 N, 87.0889 E	8.0	*triple*
4	Nuptse	7864	Himalaya	27.9675 N, 86.8869 E	0.8	*triple*
5	Chomo Lonzo	7804	Himalaya	27.9306 N, 87.1078 E	4.5	*triple, almost quad.*
6	Changtse	7543	Himalaya	28.0247 N, 86.9142 E	5.0	*quad.*
7	Chamlong	7284	Himalaya	27.7761 N, 86.9799 E	3.8	*triple*
8	Kharta Phu	7184	Himalaya	28.0637 N, 86.9767 E	6.2	*triple*
9	Baruntse	7128	Himalaya	27.8716 N, 86.9802 E		***ridge only***
10	no name	6848	Himalaya	28.0692 N, 86.8994 E	1.8	*triple*
11	Hongku Chuli	6790	Himalaya	27.8175 N, 87.0089 E	1.4	*triple*
12	Ama Dablam	6776	Himalaya	27.8616 N, 86.8614 E	3.4	*quad.*

13	Katenga	6735	Himalaya	27.7922 N, 86.8167 E	1.1	*triple*
14	Kyashar	6723	Himalaya	27.7549 N, 86.8229 E	1.8	*triple*
15	Tutse	6694	Himalaya	27.7720 N, 87.0989 E	2.9	*triple*
16	no name	6693	Himalaya	27.9576 N, 87.0165 E	3.3	*triple*
17	no name	6688	Himalaya	27.8268 N, 87.0483 E	2.4	*triple*
18	Cho Pulo	6658	Himalaya	27.9195 N, 86.9811 E	1.9	*triple*
19	no name	6598	Himalaya	27.7743 N, 86.9087 E	2.5	*triple*
20	Thamserku	6568	Himalaya	27.7899 N, 86.7852 E	3.7	*triple*
21	no name	6503	Himalaya	27.8078 N, 86.8668 E	2.8	*quad.*
22	no name	6380	Himalaya	27.8366 N, 87.1415 E	2.9	*triple*
23	Mt. Kanguru	6334	Himalaya	27.7309 N, 86.7893 E	6.2	*triple*
24	no name	6252	Himalaya	27.7273 N, 87.0074 E	25.8	*triple*
25	Tuolakangboqie	6121	Himalaya	28.0688 N, 87.1642 E	1.0	*triple*
1 peaks is ridge-only. Triple/quad = 96%. Six peaks in bold are counted above for the synthesis below.						
Summary = 255 peaks checked, 9 are constructional, 21 are ridge-only, 91% are triple-junction peaks.						

Table DR-2: Location information.

Location	Denudation rate (mm/yr)*	References
Coast Range, B.C.	0.5	1, 2
St. Elias, AK	1.5	3
Mt. Everest, Nep.	1.0	4
Alps, Swtz.	0.2	5,6
Highlands, Scot.	0.05	7,8
Chugach R., AK	0.2	9
Alaska R., AK	1.0	10
Nanga Parbat, Pak.	5.0	11,12
Tierra d. Fuego	1.0	13,14
S. Alps, NZ	3.0	15,16
Smoky Mtn., NC	0.04	17
San Gabriel Mtn., CA	2.0	18
Central Range, Taiw.	3.0	19,20
Caucasus, Russ./Georg.	0.5	21
Atlas Mtns., Morr.	0.2	22,23
Bermejo, Ecuad.	0.3	24,25
Lesser Himal., Nep.	0.3	26,27
Nanga Parbat, Pak.	1.0	11,12
Marsyandi, Nep.	3.0	28,29
King Range, CA	0.5	30

Long-term erosion rates were interpreted from combinations of references and data types spanning a range of timescales, including thermochromometry, cosmochronometry, and sediment yields. In some cases, the rates used are reported directly from papers, but in other cases data were re-interpreted to provide a simple estimate of exhumation rate. This commonly required assumption of geothermal gradient and averaging regional data or using a geologically-controlled time of onset of orogenesis and the total exhumation since that time. For example, if low-temperature apatite (U-Th)/He cooling ages have not been reset in an area with a moderately high geothermal gradient and in which exhumation began 3 Ma, the total exhumation possible is likely <1.5 km/3 Ma = <0.5 mm/yr. In other cases, exhumation rates were assumed based on the gradient of age-elevation relationships. In many cases, constraints were not available in the exact area of the ridge maps, so extrapolation from neighboring areas was required (often from multiple sources and directions). As a result, the erosion rates used here should be treated as poorly constrained (e.g. $\pm$100%). Although this is a large error, the erosion rates should be approximately correct (i.e. order of magnitude) and thus provide the means for at least a first-order comparison with ridge network metrics.

References

1) Ehlers, T.A., Farley, K.A., Rusmore, M.E., and Woodsworth, G.J., 2006, Apatite (U-Th)/He signal of large-magnitude accelerated glacial erosion, British Columbia, Geology, 34, 765-768.
2) Densmore, M.S., Ehlers, T.A., and Woodsworth, G.J., 2007, Effect of alpine glaciation on thermochronometer age-elevation profiles, Geophys. Res. Lett., 34, L02502.
3) Berger, A.L., and Spotila, J.A., 2008, Denudation and deformation of a glaciated orogenic wedge: The St. Elias orogen, Alaska, Geology, 36, 523-526.
4) Bergman, S.C., Coffield, D.Q., Donelick, R., Corrigan, J., Talbot, J., Cerveny, P., and Kelley, S., 1993, Late Cenozoic compressinoal and extensional cooling and exhumation of the Qomolagma (Mt. Everest) region, Nepal, Geol. Soc. Amer. Abstr. with Programs, 25, 6, A-176.
5) Cederbom, C.E., Sinclair, H.D., Schlunegger, F., and Rahn, M.K., 2004, Climate-induced rebound and exhumation of the European Alps, Geology, 32, 709-712.
6) Champagnac, J.D., Schlunegger, F., Norton, K., Blanckenburg, F., Abbuhl, L.M., and Schwab, M., 2009, Erosion-driven uplift of the modern Central Alps, Tectonophysics, 474, 236-249.
7) Thomson, K., Underhill, J.R., Green, P.F., Bray, R.J., and Gibson, H.J., 1999, Evidence from apatite fission track analysis for the post-Devonian burial and exhumation history of the northern Highlands, Scotland, Marine and Petroleum Geology, 16, 27-39.
8) Persano, C., Stuart, F.M., Barfod, D.N., Bishop, P., ad Brown, R.W., 2005, Constraining denudation in Scotland by using a combination of low temperature thermochronometers, Goldschmidt Conference Abstracts, Geochimica et Cosmochimica Acta, 299.
9) Spotila, J.A., and Berger, A.L., 2010, Exhumation at orogenic indentor corners under long-term glacial conditions: Example of the St. Elias Orogen, Southern Alaska, Tectonophysics, 490, 241-256.
10) Benowtiz, J.A., Layer, P., Armstrong, P., Perry, S., Haeussler, P., Fitzgerald, P., and VanLaningham, S., 2011, Spatial variations in focused exhumation along a continental-scale strike-slip fault: The Denali fault of the eastern Alaska Range, Geosphere.

11) Zeitler, P.K., Koons, P.O., Bishop, M., Chamberlain, and 16 others, 2001, Crustal reworking at Nanga Parbat, Pakistan; metamorphic consequences of thermal-mechanical coupling facilitated by erosion, Tectonics, 20, 712-728.
12) Schneider, D.A., Zeitler, P.K., Kidd, W.S.F., Edwards, M.A., 2001, Geochronology constraints on the tectonic evolution and exhumation of Nanga Parbat, western Himalayan syntaxis, revisited, J. Geology, 109, 563-583.
13) Thomson, S.N., 2002, Late Cenozoic geomorphic and tectonic evolution of the Patagonian Andes between latitudes 42˚S and 46˚S: An appraisal based on fission-track results from the transpressional intra-arc Liquiñe-Ofqui fault zone, Geol. Soc. Amer. Bull., 114, 1159-1173.
14) Thomson, S.N., Brandon, M.T., Tomkin, J.H., Reiners, P.W., Vasquez, C., and Wilson, N., 2010, Glaciation as a destructive and constructive control on mountain building, Nature, 467, 313-317.
15) Little, T.A., Cox, S., Vry, J.K., and Batt, G., 2005, Variations in exhumation level and uplift rate along the oblique-slip Alpine fault, central Southern Alps, New Zealand, Geol. Soc. Amer. Bull., 117, 707-723.
16) Batt, G.E., Braun, J., Kohn, B.P., and McDougall, I., 2000, Thermochronological analysis of the dynamics of the Southern Alps, New Zealand, Geol. Soc. Amer. Bull., 112, 250-266.
17) Matmon, A., Bierman, P., Larsen, J., Southworth, S., Pavich, M., and Caffee, M., 2003, Temporally and spatially uniform rates of erosion in the southern Appalachian Great Smoky Mountains, Geology, 31, 155-158.
18) Spotila, J.A., House, M.A., Blythe, A.E., Niemi, N.A., Bank, G.C., 2002. Controls on the erosion and geomorphic evolution of the San Bernardino and San Gabriel Mountains, Southern California, in Contributions to crustal evolution of the Southwestern United States, Spec. Pap. Geol. Soc. Am., 365, 205-230.
19) Beyssac, O., Simoes, M., Avouac, J.P., Farley, K.A., Chen, Y.-G., Chan, Y.-C., and Goffe, B., 2007, Late Cenozoic metamorphic evolution and exhumation of Taiwan, Tectonics, 26, TC6001.
20) Fuller, C.W., Willett, S.D., Fisher, D., and Lu, C.Y., 2006, A thermomechanical wedge model of Taiwan constrained by fission-track thermochronometry, Tectonophysics, 425, 1-24.
21) Vincent, S.J., Carter, A., Lavrishchev, V.A., Rice, S.P., Barabadze, T.G., and Hovius, N., 2010, The exhumation of the western Greater Caucasus: a thermochronometric study, Geol. Mag., 148, 1-21.
22) Balestrieri, M.L., Moratti, G., Bigazzi, G., and Algouti, A., 2009, Neogene exhumation of the Marrakech High Atlas (Morocco) recorded by apatite fission-track analysis, Terra Nova, 21, 75-82.
23) Delcaillau, B., Laville, E., Amhrar, M., Namous, M., Dugue, O., and Pedoja, K., 2010, Quaternary evolution of the Marrakech High Atlas and morphotectonic evidence of activity along the Tizi n'Test fault, Morocco, Geomorphology, 118, 262-279.
24) Spikings, R.A., Winkler, W., Hughes, R.A., and Handler, R., 2005, Thermochronology of allochthonous terranes in Ecuador: Unravelling the accretionary and post-accretionary history of the Northern Andes, Tectonophysics, 399, 195-220.
25) Spikings, R.A., and Crowhurst, P.V., 2004, (U-Th)/He thermochronometric constraints on the late Miocene-Pliocene tectonic development of the northern Cordillera Real and the Interandean Depression, Ecuador, J. S. Amer. Earth Sci., 17, 239-251.
26) Patel, R.C., Kumar, Y., Lal, N., and Kumar, A., 2007, Thermotectonic history of the Chiplakot Crystalline Belt in the Lesser Himalaya, Kumaon, India: Constraints from apatite fission-track thermochronology, J. Asian Earth Sci., 29, 430-439.
27) Herman, F., Copeland, P., Avouac, J.-P., and Bollinger, L., 2010, Exhumation, crustal deformation, and thermal structure of the Nepal Himalaya derived from the inversion of thermochronological and thermobarometric data and modeling of the topography, J. Geophys. Res., 114, B06407.
28) Lave, J., and Avouac, J.P., 2001, Fluvial incision and tectonic uplift across the Himalayas of central Nepal, J. Geophys. Res., 106, 26,561-26,591.
29) Blythe, A.E., Burbank, D.W., Carter, A., Schmidt, K., Putkonen, J., 2007, Plio-Quaternary exhumation history of the central Nepalese Himalaya: 1. Apatite and zircon fission track and apatite (U-Th)/He analyses, Tectonics, 26, TC3002.
30) Dumitru, T.A., 1991, Major Quaternary uplift along the northermost San Andreas fault, King Range, northwestern California, Geology, 19, 526-529.

Table DR-3: Results from ridge profiles.

Location	DJ=pks.	Max=DJ-pks.	Avg. slope	Ψ_1	Ψ_2
		Glacial			
Coast Range, B.C.	55%	31%	10.7˚	0.24	1.92
St. Elias, AK	73%	32%	9.1˚	0.20	1.74
Mt. Everest, Nepal	83%	38%	19.3˚	0.20	3.20
Alps, Switzerland	71%	43%	10.9˚	0.13	2.05
Highlands, Scotland	88%	23%	6.7˚	0.21	1.45
Average	*74%*	*33%*	*11.3˚*	*0.20*	*2.07*
		Fluvial			
Smoky Mtn., NC	68%	59%	1.6˚	0.32	1.22
San Gabriel Mtn., CA	68%	50%	9.3˚	0.32	1.76
Central Range, Taiwan	72%	52%	7.1˚	0.30	1.49
Caucasus, Georgia	73%	62%	8.1˚	0.25	1.62
Atlas Mtns., Morocco	62%	35%	7.8˚	0.30	1.51
Average	*69%*	*52%*	*6.8˚*	*0.30*	*1.52*
Overall average	**72%**	**43%**	**9.0˚**	**0.25**	**1.80**

DJ=peaks: percent of divide junctions that occur at peaks.
Max=DJ-peaks: percent of all elevation maxima that are divide-junction peaks.
Avg. slope: slope of the ridge along the profile.
Ψ_1: topographic roughness #1; unit distance (relative to entire profile over which half of the ridge's relief is attained (low value = rougher).
Ψ_2: topographic roughness #2; vertical irregularity (akin to sinuosity) of profile, measured at 8x vertical exaggeration (high value = rougher).

Table DR-4: Results from ridge maps.

Location	ρ (km^{-1})	γ (km^{-2})	χ (km^{-1})	Sin.	Relief (m)	Denud.
			Glacial			
Coast Range, British Co.	0.358	0.029	0.080	1.33	4019	0.5
St. Elias, AK	0.236	0.018	0.078	1.23	2502	1.5
Mt. Everest, Nepal	0.285	0.024	0.083	1.22	7450	1.0
Alps, Switzerland	0.268	0.022	0.084	1.23	3920	0.2
Highlands, Scotland*	0.279	0.014*	0.050*	-	1060	0.05
Chugach Range, AK*	0.244	0.012*	0.051*	1.35	2139	0.2
Alaska Range, AK	0.254	0.021	0.082	1.40	5493	1.0
Nanga Parbat, Pakistan	0.308	0.033	0.107	1.21	5526	5.0
Tierra d. Fuego	0.238	0.017	0.073	1.35	2520	1.0
S. Alps, New Zealand	0.269	0.025	0.093	1.21	3680	3.0
Average	**0.274**	**0.022**	**0.078**	**1.28**		
*R^2 vs. relief***	*0.11*	*0.44*	*0.46*	*0.07*		
*R^2 vs. denudation rate***	*0.03*	*0.48*	*0.63*	*0.25*		
			Fluvial			
Smoky Mtn., NC	0.235	0.019	0.082	1.19	1750	0.04
San Gabriel Mtn., CA	0.311	0.025	0.080	1.24	2580	2.0
Central Range, Taiwan	0.302	0.028	0.093	1.27	3750	3.0
Caucasus, Georgia	0.299	0.028	0.094	1.18	3615	0.5
Atlas Mtns., Morocco*	0.282	0.016*	0.055*	1.19	3367	0.2
Bermejo, Ecuador*	0.304	0.018*	0.058*	1.24	3540	0.3
Lesser Himalaya, Nepal	0.257	0.017	0.065	1.23	4360	0.3
Nanga Parbat, Pakistan	0.307	0.024	0.078	1.20	3700	1.0
Marsyandi, Nepal	0.236	0.016	0.068	1.20	7150	3.0
King Range, CA	0.272	0.019	0.070	1.18	1113	0.5
Average	**0.281**	**0.021**	**0.074**	**1.21**		
*R^2 vs. relief***	*0.05*	*0.04*	*0.03*	*0.03*		
*R^2 vs. denudation rate***	*0.01*	*0.11*	*0.12*	*0.27*		
Overall average	**0.278**	**0.021**	**0.076**	**1.25**		

ρ: ridge density, or total length of ridges divided by area.
γ: junction density, or total number of divide junctions divided by map area.
χ: divide connectivity, number of divide junctions per unit length of ridges.
Sin: sinuosity, irregular ridge length divided by linear ridge length.
Denud.: long-term denudation rate, mm/yr (see Table DR-2).
**Note anomalously poor divide connectivity for these four outliers; see text.*
***Correlation coefficients based on basic regressions between ρ, γ, χ, and sinuosity vs. relief and denudation rate. Plots not shown (no strong correlations).*

Figure DR-1

The geometry of peaks. A) Hillslopes with parallel trends, even at the angle of repose (hillslope angle = δ), will create a horizontal ridgeline. B) Oblique hillslopes (obliquity angle = γ) will generate an inclined ridgeline (ridgeline angle = θ). In this example, hillsides at the angle of repose (δ=34˚) that intersect by 24˚ (γ) will generate a ridgeline slope (θ) of 8˚. C) Plot of increasing ridgeline slope with increasing obliquity between hillsides, for select hillslope gradients. D) Conceptual diagram illustrating how the competition of abutting basins, represented by the relative horizontal velocity of the headwall or channel head (U_a vs. U_b), should shape the intervening ridgeline. In this case, U_a>U_b requires that the ridge migrate from left to right, although it is easy to envision a spectrum of possible scenarios. E) Illustration of peak "prominence". Prominence is defined as the relative height of a peak above the lowest contour that underlies it and no taller peak. The three peaks shown have prominence defined by the arrows. Note that although the middle peak may be very high, its prominence is simply the relative height of the peak above the saddle to its right. F) Two example ridgeline profiles with different scales of peak prominence. The parabolic ridge on the left has many peaks of small prominence, but only one peak that exceeds the prominence threshold indicated by the bar. The ridge on the right has lower mean elevation, but a higher number of prominent peaks, because of the low saddles. G) Illustration of measurement of third-shortest contributing divide. For the divide-junction circled, the path shown by dashed line would be measured as the third shortest divide. It is shorter than divides #1 and #2, but follows the primary divide leaving the junction as opposed to following a shorter secondary divide (e.g. #3) down to base level.

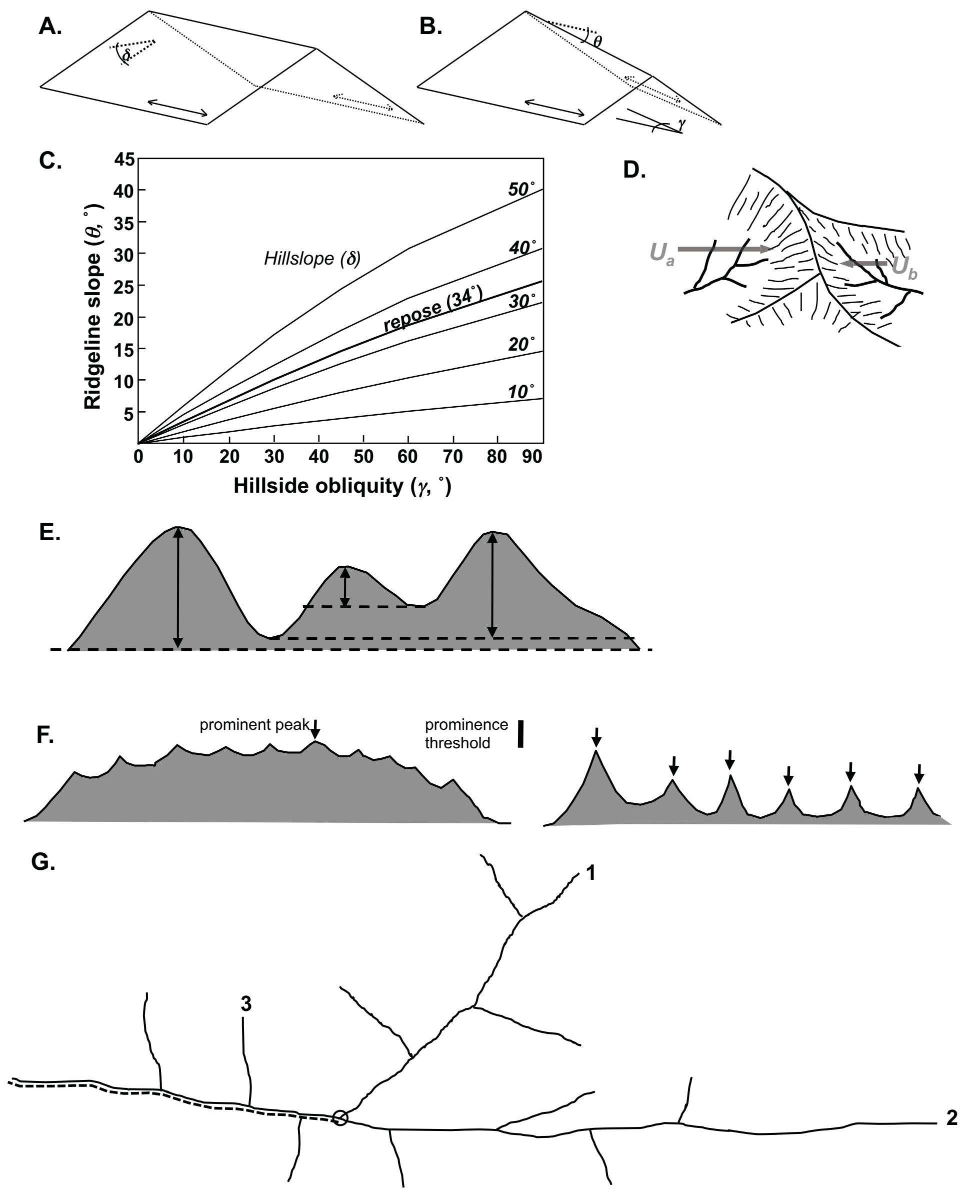

Figure DR-2

Additional example images of prominent pyramidal peaks that occur at the junction of major ridges. The first five are from glacial settings, whereas Baden Powell, Yushan, and Twin Peaks are fluvial. Scales and aspects of each image are variable, as noted. Images were captured from GoogleEarth. Numbers refer to the group and peak number in Table DR-I.

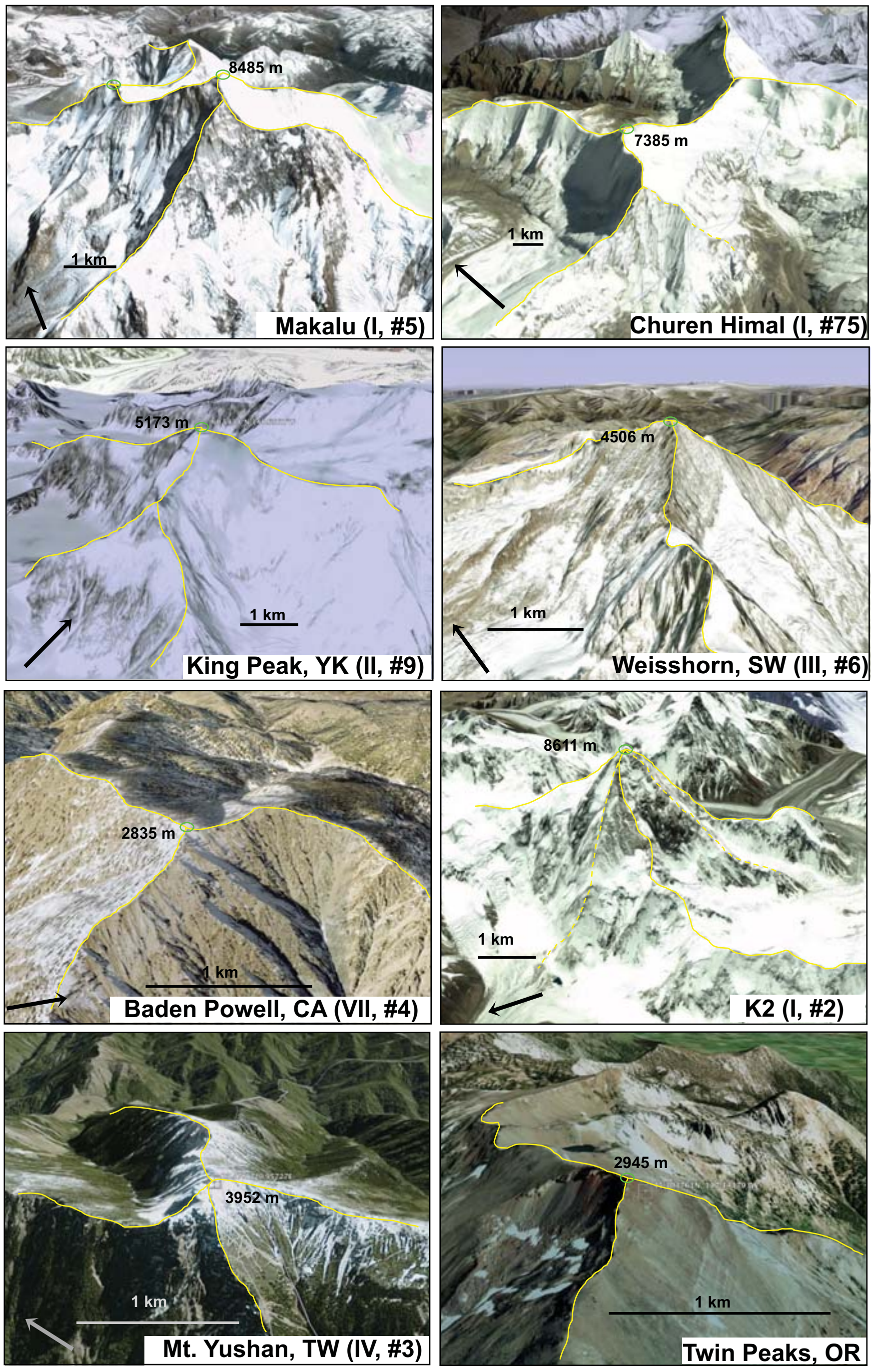

Figure DR-3

Examples of pominent peaks identified in the global survey (numbers provided refering to Table DR-1) that would not classify as divide-juncton. These are characteristic examples of ridge-only peaks. In some cases, it may appear that a third contributing ridge exists, but on close examination these divides do not come within 0.2 km of the peak itself. All examples are from the Himalaya: A) Broad Peak (Group I, #12), B) Teram Kangri (Group I, #59), C) Baintha Brakk (Group 1, #90), D) Muztagh Tower (Group I, #94) (see Table DR-1). Scale bar represents 1 km in all cases.

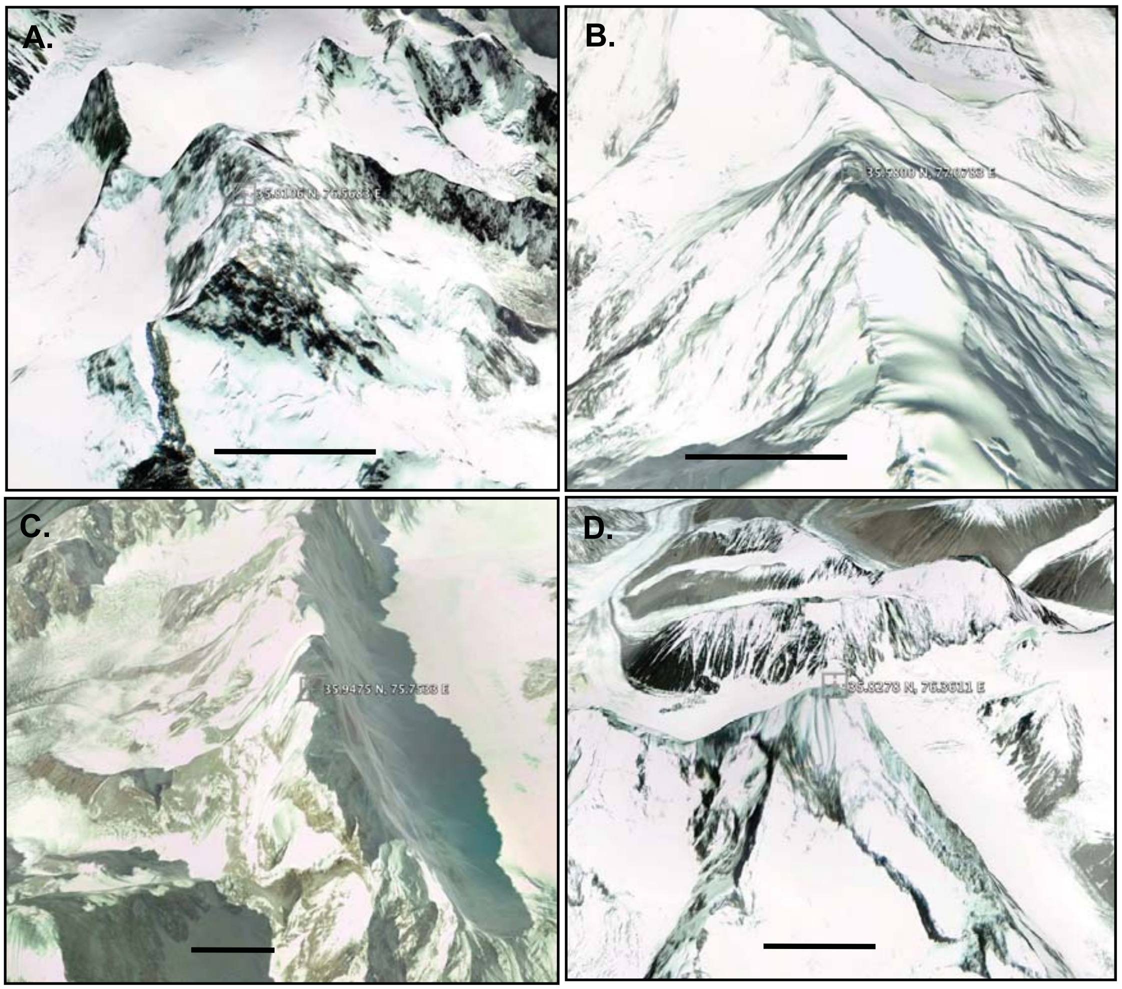

Figure DR-4a Summary of all 10 ridgeline maps in fluvial locations. Locations are indicated by coordinates of highest peak in each area (triangle). An asterisk indicates that the peak is not a divide-junction peak at the scale of these maps; that is, it does not co-locate with a third-shortest contributing divide that is >5 km long (note that this differes from the criteria used in Table 1, DR-1). North is vertical on all maps except Ecuador. The dashed lines enclosing the mapped areas are in some cases the boundary of a small ranges, but in others is arbitrary sampling of a larger area (normally following valleys). Red divides are profiles in Figure DR-5.

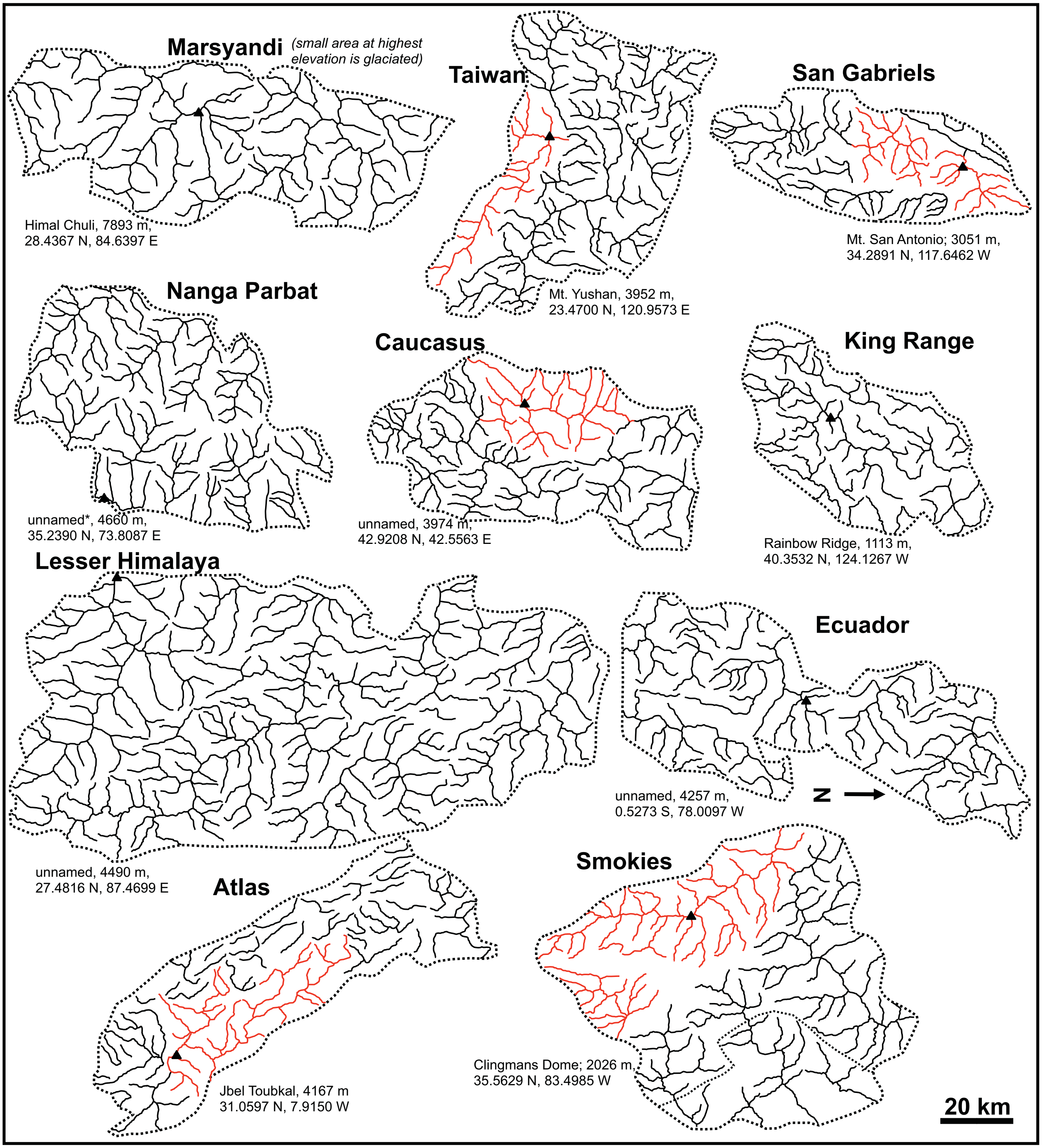

Figure DR-4b Summary of all 10 ridgeline maps in glacial locations.

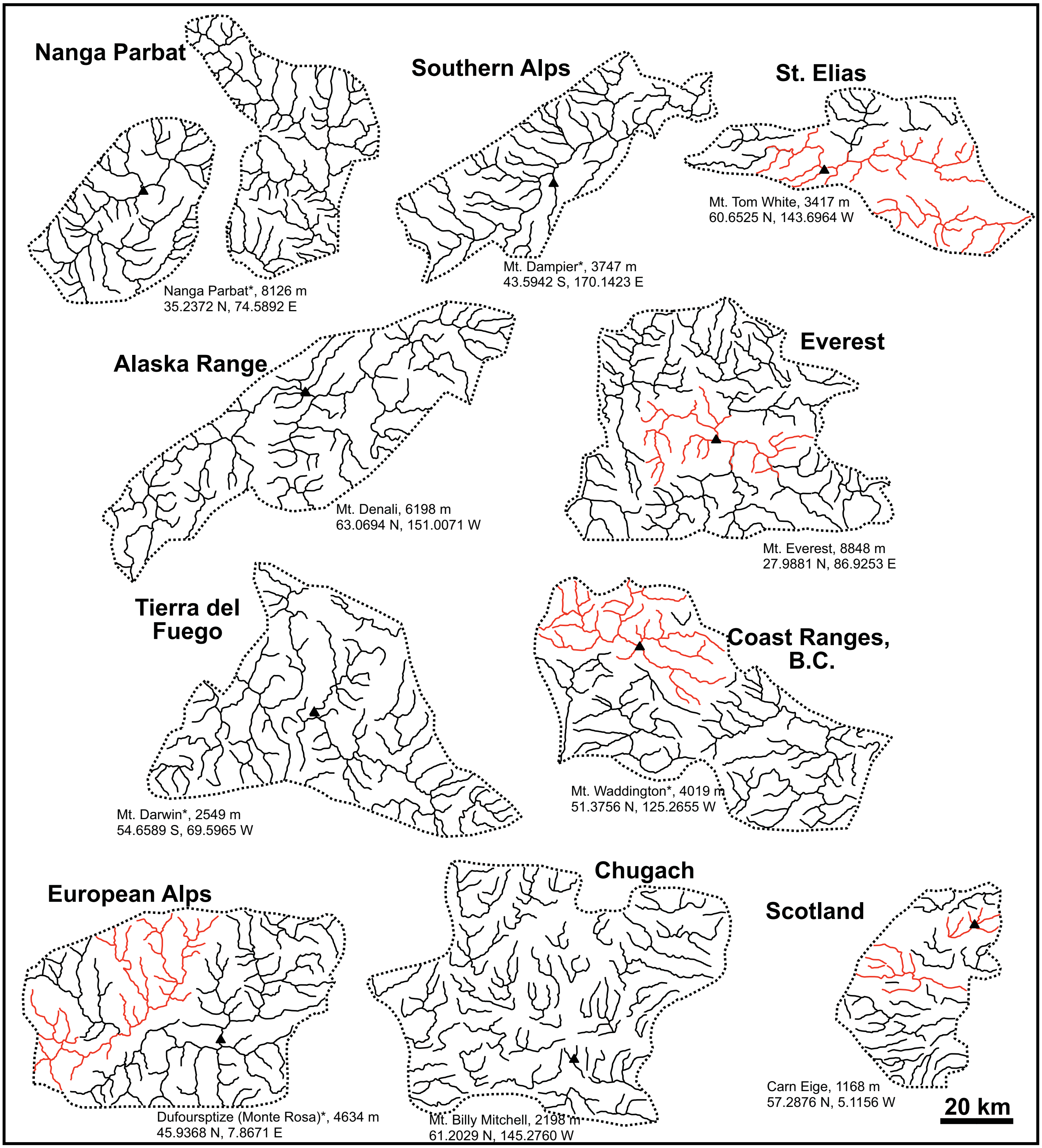

Figure DR-5 All ridgeline profiles constructured in this study. Profiles are exaggerated 7.7x and are from five fluvial and five glacial areas, as listed in Table 2. Note that these are not familiar swath or linear elevation profiles, but rather the elevation along the irregular line of mapped ridge. Secondary ridges that join the primary ridge from the flank are also plotted, color coded for direction from which they approach. The location of peaks and divide junctions (DJs) are indicated (green circle = peak; yellow box = triple junction; organge box = quadruple juction). Statistics are listed at the side and in Table 2. Arrows show the location of the four highest prominent peaks in each area.

Smoky Mtns., secondary, fluvial

final statistics in Table 2 are weighted average of the two profiles.

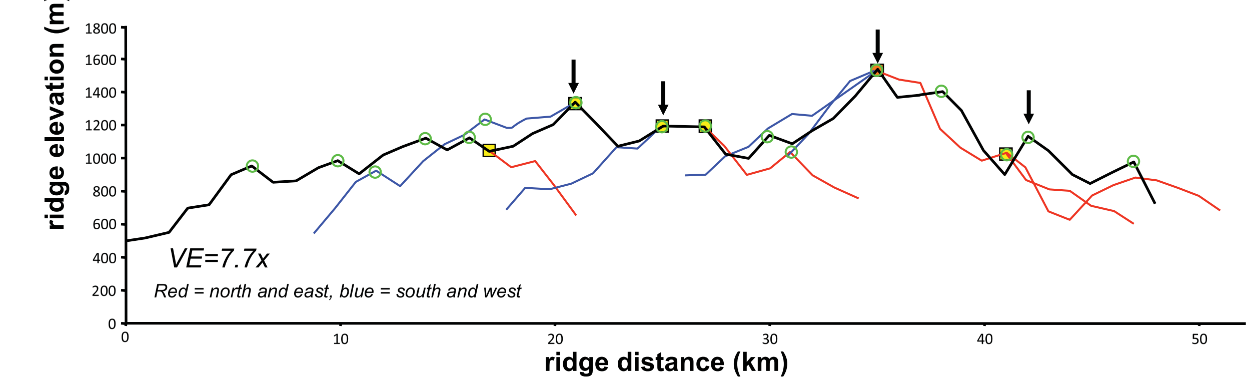

DJs that correspond to peaks = 7/9 = 78%
of 16 peaks, 44% are DJs
3 of 4 biggest peaks are DJs
Avg. ridge elev. = 998 m
Avg. DJ elev. = 1206 m (20.8% higher)
St. dev. of ridge elev. = ±225 m (± 22.5%)

DJs that correspond to peaks = 20/31 = 66%
of 30 peaks, 67% are DJs
4 of 4 biggest peaks are DJs
Avg. ridge elev. = 1343 m
Avg. DJ elev. = 1652 m (23.0% higher)
St. dev. of ridge elev. = ± 320 m (± 23.8%)

Smoky Mtns., Clingmans Dome

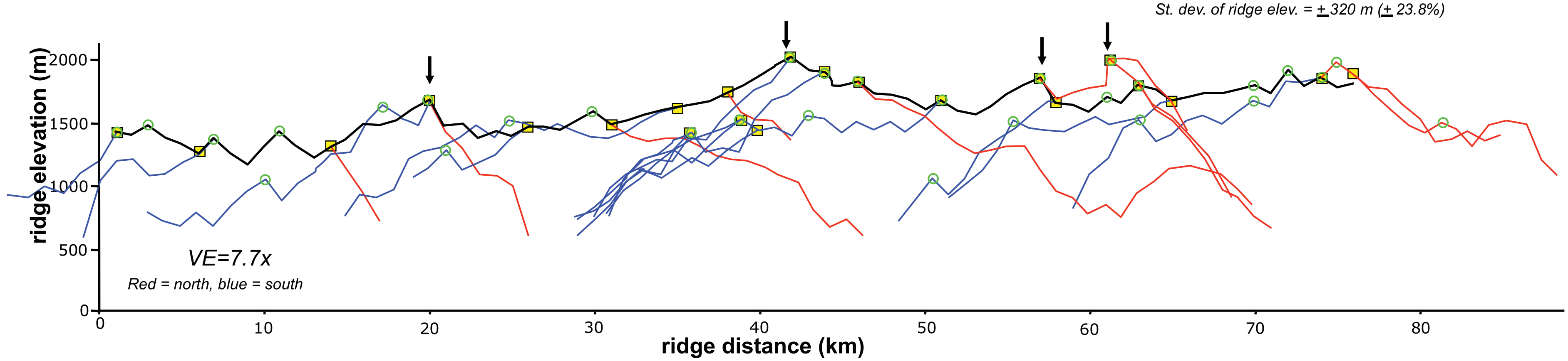

Figure DR-5, cont.

final statistics in Table 2 are weighted average of the two profiles.

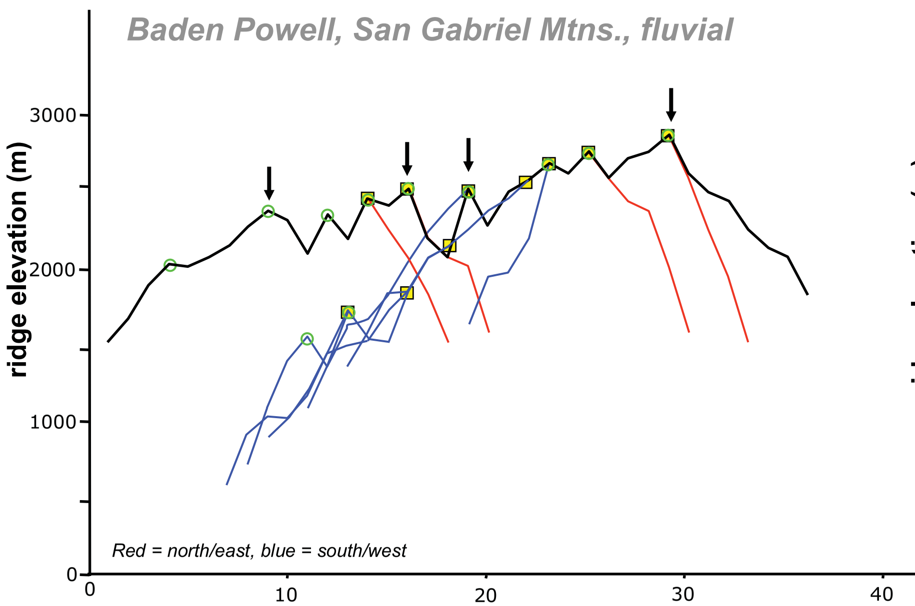

DJs that correspond to peaks = 7/10 = 70%
of 11 peaks, 64% are DJs
3 of 4 biggest peaks are DJs
Avg. ridge elev. = 1990 m
Avg. DJ elev. = 2412 m (21.2% higher)
St. dev. of ridge elev. = ±513 m (± 25.8%)

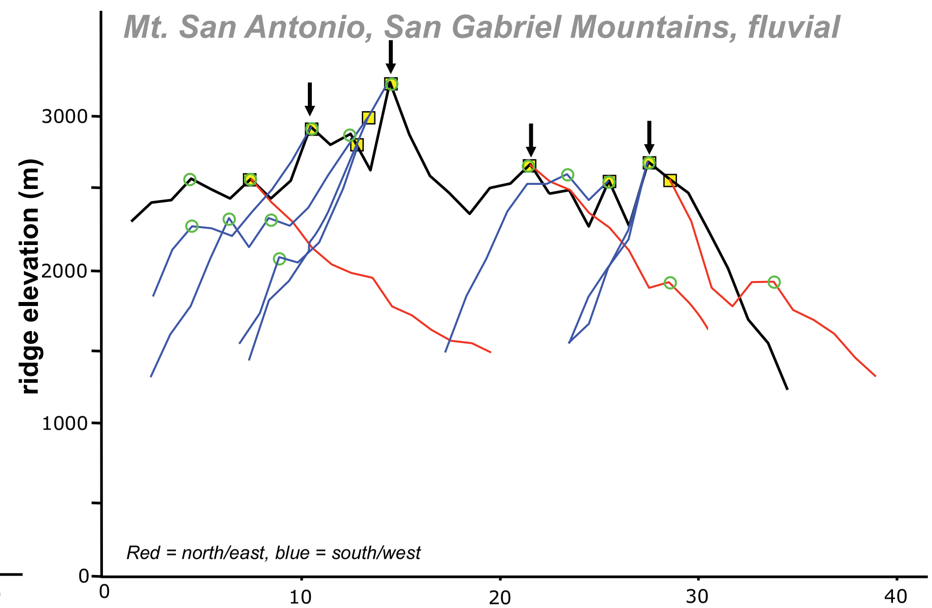

DJs that correspond to peaks = 6/9 = 67%
of 15 peaks, 40% are DJs
4 of 4 biggest peaks are DJs
Avg. ridge elev. = 2219 m
Avg. DJ elev. = 2786 m (25.6% higher)
St. dev. of ridge elev. = ±451 m (± 20.3%)

Figure DR-5, cont.

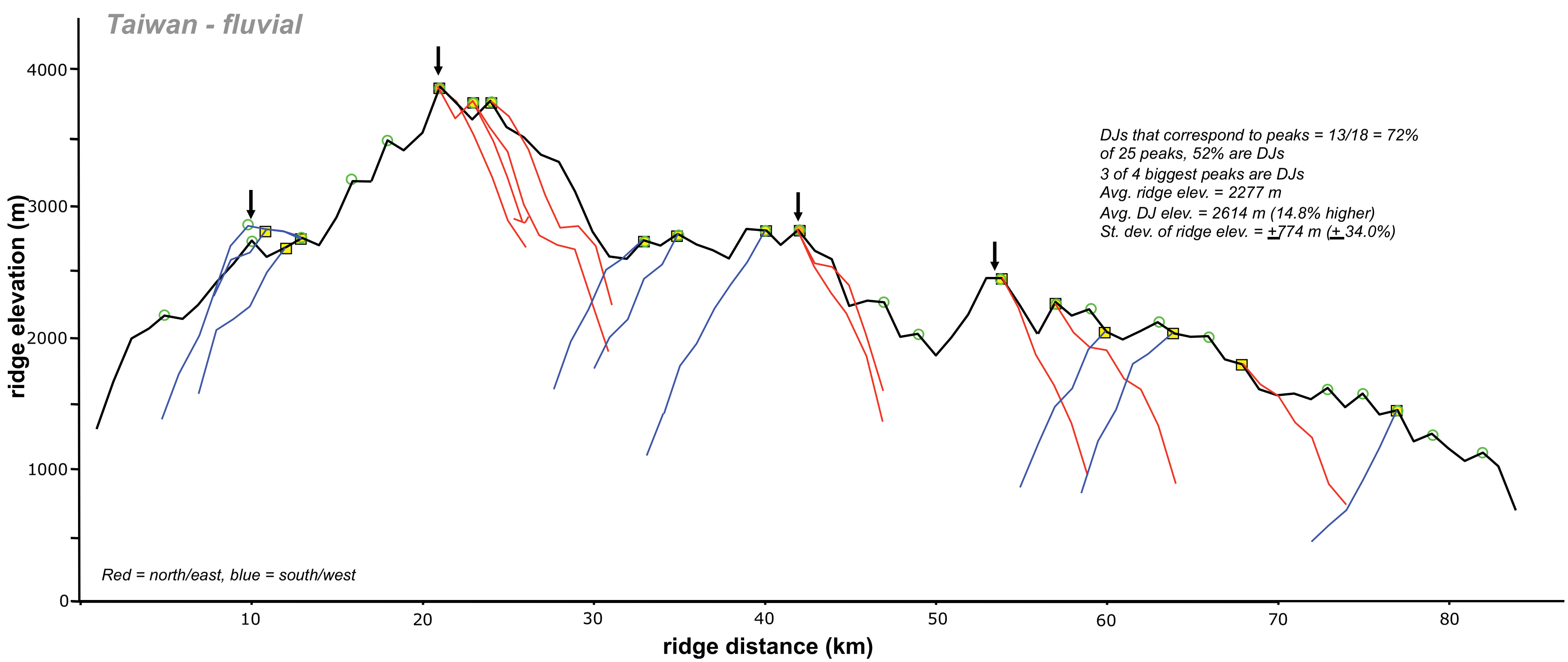

Figure DR-5, cont.

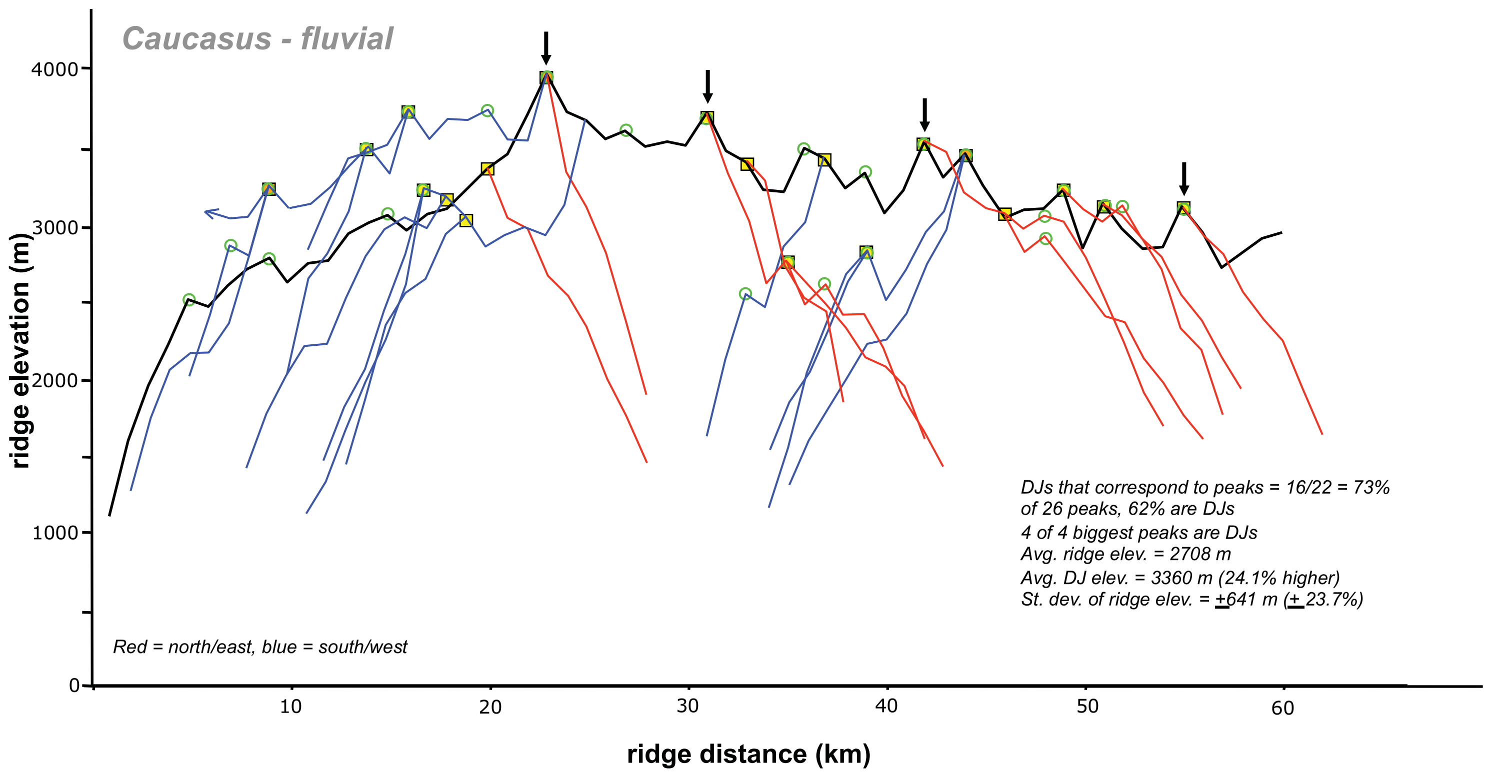

Figure DR-5, cont.

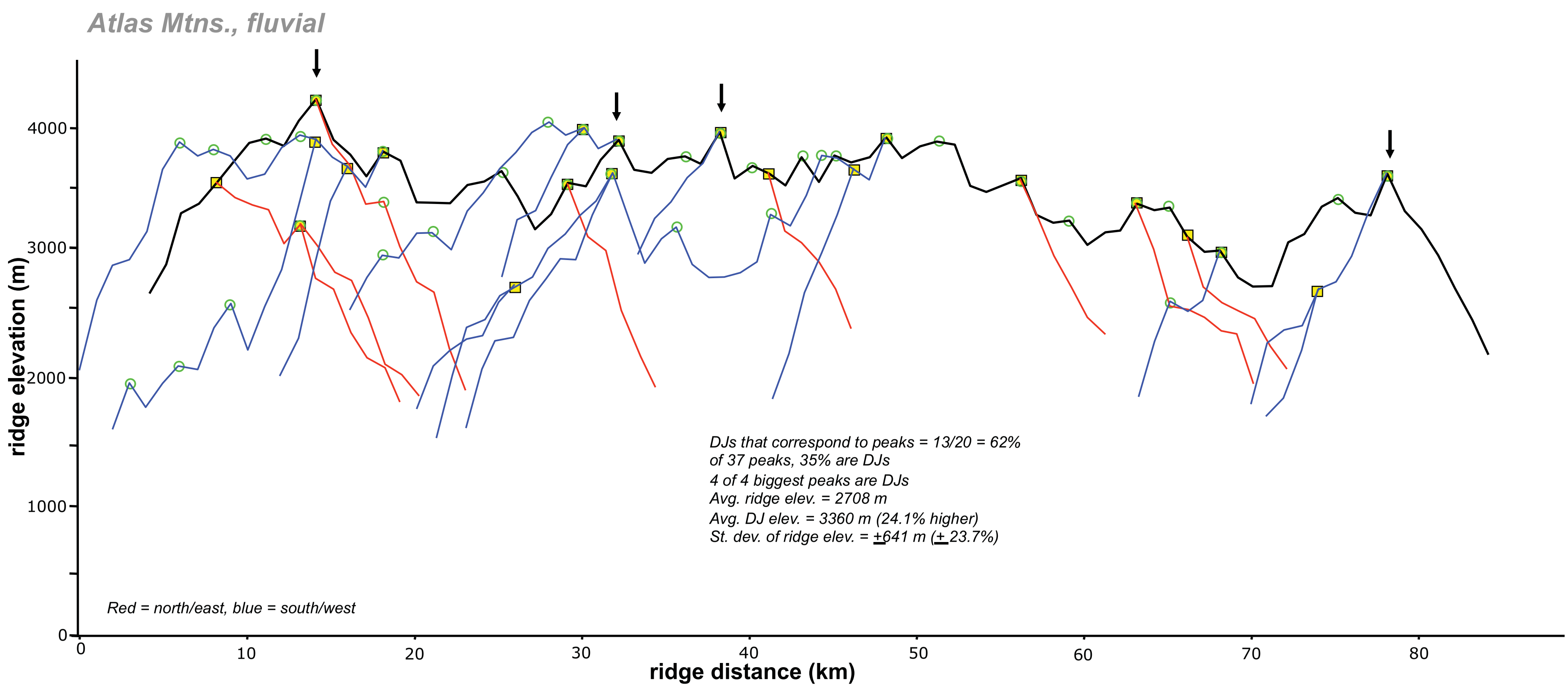

Figure DR-5, cont.

final statistics in Table 2 are weighted average of the two profiles.

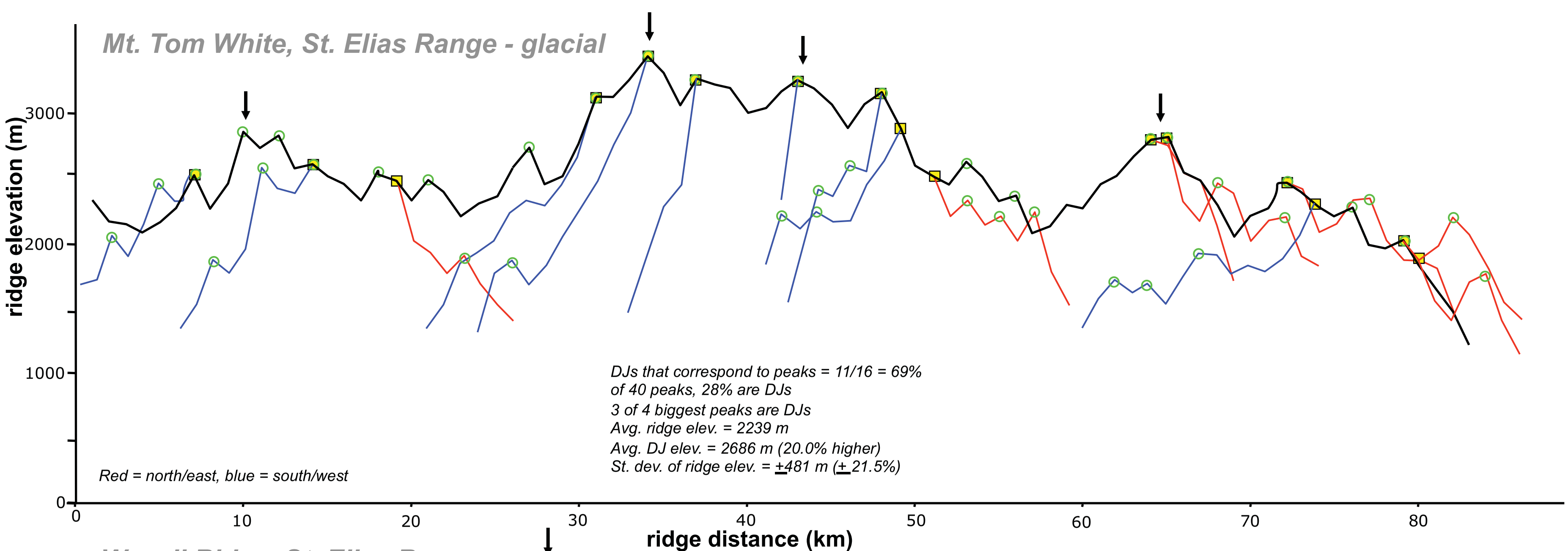

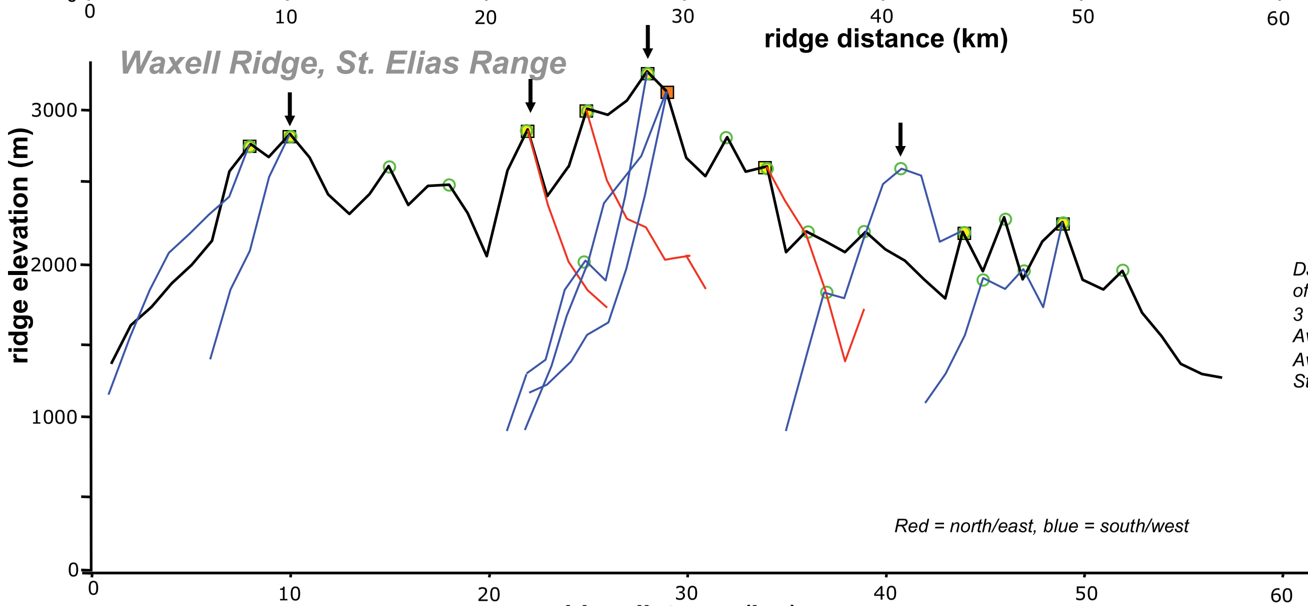

Figure DR-5, cont.

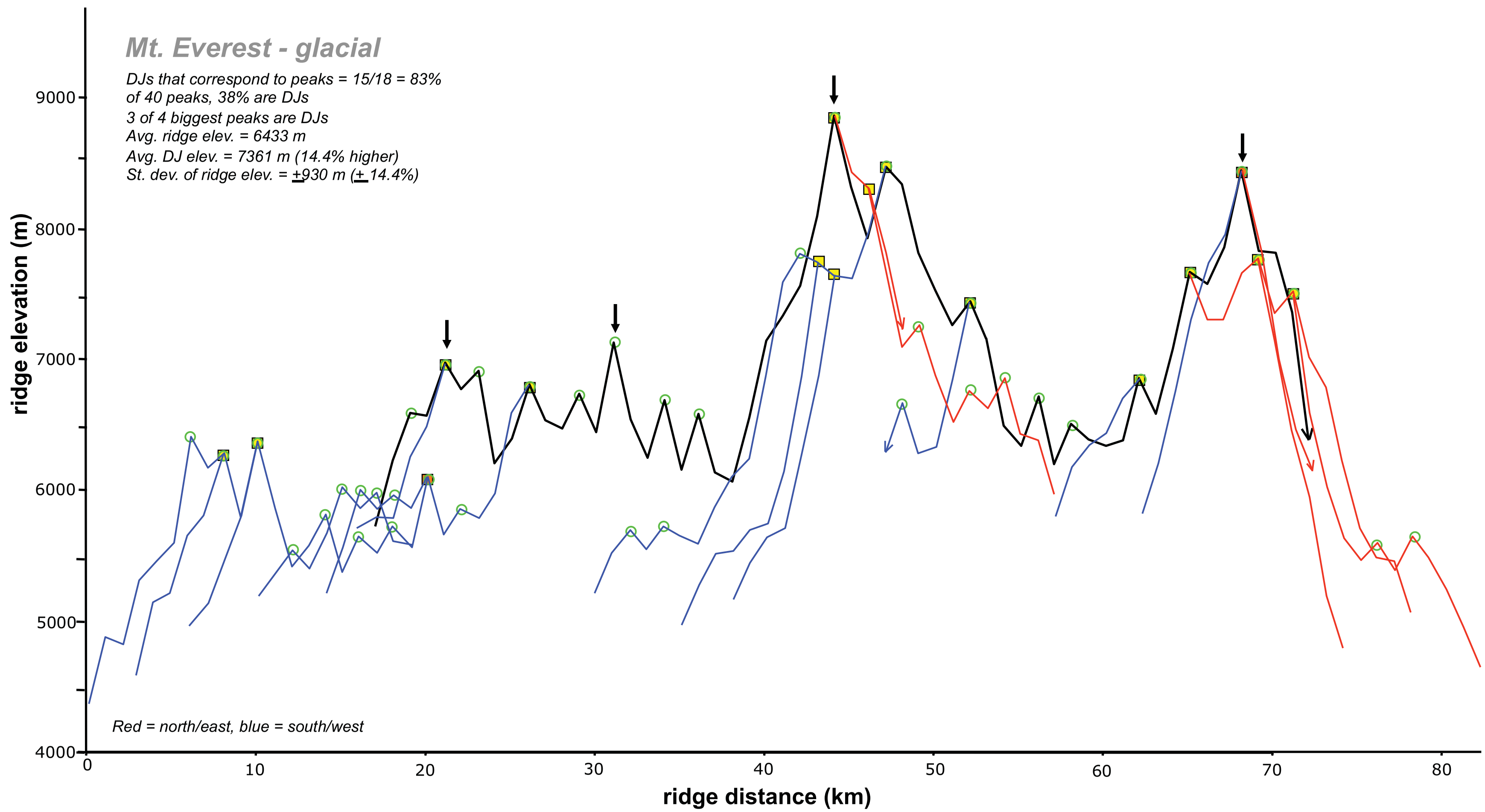

Figure DR-5, cont.

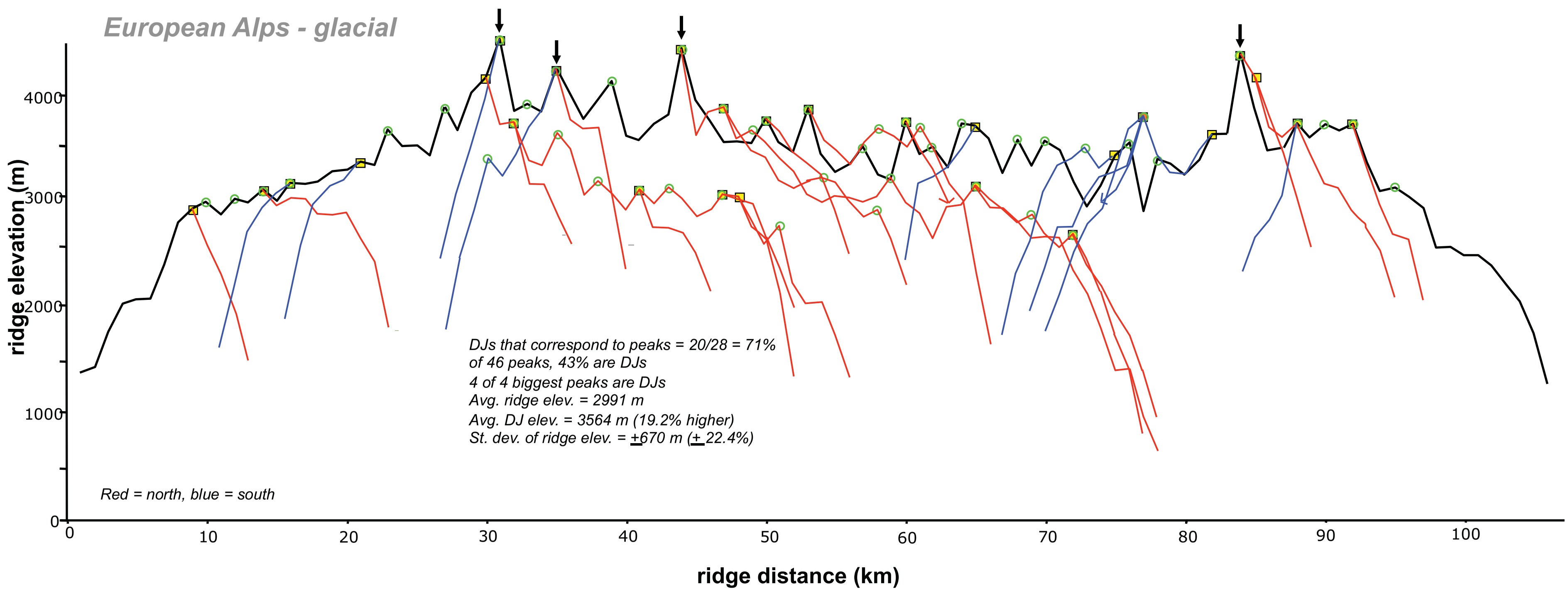

*plotted at a slightly smaller scale than the other 9 profiles, to fit onto one page

Figure DR-5, cont.

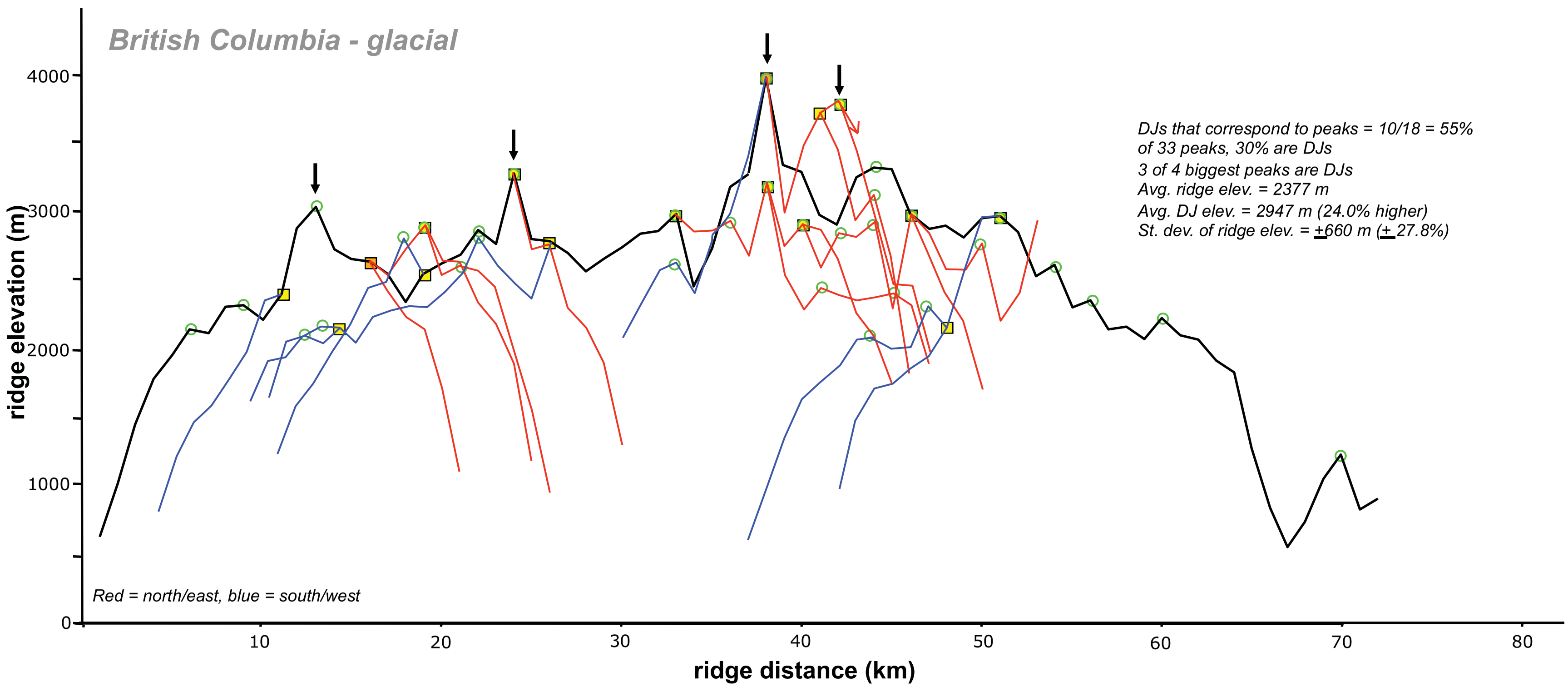

Figure DR-5, cont.